FLEXENER – TECHNICAL REPORT

A review of methods for the estimation of inertia and its distribution

Aurelio García, Álvaro Ortega, Luis Rouco, Lukas Sigrist

Prepared by IIT for i-DE

October 2021

Version: 1.0

This study is funded by Centro para el Desarrollo Tecnológico Industrial (CDTI) and supported by Ministerio de Ciencia e Innovación, Project MIG-20201002.

CONTENT

1 Introduction

Inertia is a physical property of rotating machines and it denotes the resistance of the rotor speed to torque variations. Rotating machines can be found in conventional generating units such as thermal and hydro generating units using synchronous generators. The inertia is technology dependent and takes typical values in *per unit*. Induction-motor driven loads also involve rotating machines. Although wind generators make use of rotating machines to converter kinetic into electrical energy, these are coupled to the grid by a stage of electronic power converters, either through the stator or the rotor. The control of these converters controls the rotating speed according to the maximum power point (MPP), decoupling rotor speed from grid-side disturbances (non-synchronous generators). Nonetheless, wind generators could provide an inertial response through appropriate controls. A similar remark applies to variable speed electric drives (VFD) that are connected to the grid by a stage of electronic power converters.

System inertia refers to total inertia of a system. It is, at least, equal to the sum of the inertia values of the connected rotating machines, dominated in the past by the inertias of large conventional generating units. System inertia is related to the hypothesis of a uniform frequency within a system by neglecting inter-machine oscillations, which holds true in steady state but not during transients. This system frequency is given by the frequency of the center of inertia (COI). In this regard, **system inertia opposes frequency changes when active power balances occur**.[1] It affects to a large extent the system-wide average rate-of-change of frequency (ROCOF) at the time of occurrence of the disturbance, but also the frequency nadir and frequency recovery [2]. By assuming, for instance, invariant primary frequency control characteristics, the reduction of system inertia leads to steeper ROCOF and lower frequency nadir for a given disturbance. Note that the increasing penetration of non-synchronous generation does not only affect system inertia but also primary frequency control characteristic if the non-synchronous generation does not contribute to inertia emulation and primary frequency control. Currently, conventional generating units still provide most of the inertia and primary frequency control, but they are gradually being replaced by non-synchronous generation in the generation dispatch. **The reduction of system inertia could lead to unnecessary underfrequency load shedding (UFLS), activate ROCOF-based anti-islanding protection schemes of distributed generation, etc.** In this regard, (Mehigan et al. 2020) has studied the impact of system inertia constraints on operation planning of five synchronous areas of Continental Europe. Imposing smaller largest admissible ROCOF values tends to increase costs and non-synchronous generation curtailment, where the effect is stronger in smaller weakly interconnected systems than in larger ones. Inertia emulation could however further increase non-synchronous generation penetration in already low-inertia systems. Furthermore, existing synchronous generators transformed into synchronous compensators could provide additional support.

[1] In *per unit,* torque and power variations are approximately equal as long as speed variations are small.

[2] Frequency nadir refers to the minimum frequency value after an active power unbalance. Frequency recovery denotes here the process during which frequency increases and regains its nominal value after have reached its nadir. Physical inertia opposes frequency recovery in the same way it opposes frequency drop.

(Nikolic and Negnevitsky 2019) presents field tests involving synchronous compensators in King Island, Australia.

The interpretation of the system inertia as the system frequency's opposition to change when there are active power unbalances can be further extended to include the contribution to inertial response of non-synchronous generation and even load. **The term *effective inertia* has been coined to include virtual or emulated inertia and voltage- and frequency-dependency of loads**. The effective inertia actually relates active power variations with ROCOF. Indeed, non-synchronous generation could hold back a certain power margin by operating at a sub-optimal power point (deloaded operation), that could be activated by appropriate controls. The exact activation depends on whether the grid-side electronic power converter operates in grid-following or grid-forming mode. In addition, wind generators can also extract kinetic energy stored in the inertia of their rotors. Under this control, the wind generator operates at its MPP, but when needed, the active power set point is increased temporarily which slows down the rotor speed of the wind generator, releasing stored energy. Finally, an active power disturbance is usually accompanied by a voltage variation, that nearly immediately affects power consumption of loads (e.g., torque of induction motors depends on the square of the stator voltage).

Not only the total amount of inertia is important, but also its distribution within a system. **System inertia is not uniformly distributed among the buses of a system**. Different generation technologies at different locations have different inertia values and they inherently cause an uneven inertia distribution. In case of non-synchronous generation providing inertial response (e.g., wind generators through deloaded operation or temporary overspeed), the inertia further depends on the availability of the primary resource. An uneven distribution of the system inertia can lead to local problems (contrary to system-wide problems). The term **local inertia phenomenon** refers to a power system with an uneven distribution of inertia across the entire system (Osbouei et al. 2019). The distribution of the inertia affects local ROCOF, inter-area oscillations and critical clearing times, but frequency nadir is affected by the system inertia level rather than by the distribution of the inertia. In this regard, (Osbouei et al. 2019) studies the impact of local inertia phenomenon on small-signal stability (inter-area oscillations), transient stability (critical clearing times) and frequency stability (local ROCOF, nadir) under different inertia distribution scenarios between Scotland, and Wales and England. Finally, (Mehigan et al. 2020) concludes that although a synchronous area as a whole might have sufficient inertia, amounts at country-level might be insufficient, being a risk in case of system splitting events.

Estimating system inertia is basically a model-identification problem. Non-parametric and parametric model-identification approaches exist. Parametric identification approaches initially start from a given mathematical structure of the model. Mathematical models can be classified into white-box, grey-box, and black-box model. White-box models mathematically describe the physical relations of an element and its associated controls, whereas black-box models only describe the input-output relations without taking into account the internal physical and control-based relations. Grey-box models combine white-box and black-box models, i.e., approximate mathematical formulations (usually of reduced-order) are combined with generic parametrization of input-output relations. Most of the reviewed methods of inertia estimation make use of a parametric model identification.

This report reviews the technical literature with respect to inertia estimation methods. Section 2 reviews concepts and provides definitions on physical inertia, system inertia, and emulated inertia. Section 3 provides an overview and insight of the transient response of the system in terms of generator speeds to active power unbalances. Most methods on inertia estimation make use of the different phases during the power system transient. The review of the inertia estimation methods is presented in section 4, whereas section 5 discusses the methods and their application to distribution system. Indeed, the amount of distributed generation and noticeably non-synchronous distributed generation connected to distribution systems is increasing. Their contribution to system inertia is thus increasing as well. Although inertia reduction is mostly considered a system-wide issue and inertial response therefore belongs to the ancillary services managed by the system operator (Kryonidis et al. 2021), **distribution system operators need tools, among others, for monitoring of inertial response and estimation of inertia within their systems.**

2 Concepts and definitions

2.1 Physical inertia

Inertia is a physical property of rotating machines. Inertia quantifies the resistance of the rotor speed to change when torque variations occur. In *per unit,* torque and power variations are approximately equal. The rotor dynamics of a generating unit are driven by Newton's second law for rotation.

$$J_g \cdot \frac{d\Omega_g}{dt} = T_{mg} - T_{eg} - K_{Dg} \cdot \left(\Omega_g - \Omega_{B,g}\right) \tag{1}$$

where J_g is the moment of inertia, Ω_g the rotor speed, T_{mg} and T_{eq} the mechanical and electrical torque, respectively, and K_{dg} the damping coefficient. If the equation is written in *per unit:*

$$\frac{J_g \cdot \Omega_{B,g}^2}{M_{B,g}} \cdot \frac{d\omega_g}{dt} = t_{mg} - t_{eg} - \frac{K_{Dg} \cdot \Omega_{B,g}^2}{M_{B,g}} \cdot \left(\omega_g - 1\right) \tag{2}$$

where $\Omega_{B,g}$ and $M_{B,g}$ are the rated speed and power. Since power is related to torque through speed $p = t \cdot \omega_g$, the rotor dynamics can be written as follows:

$$2H_g \cdot \frac{d\omega_g}{dt} = p_{mg} - p_{eg} - D_g \cdot \left(\omega_g - 1\right) \tag{3}$$

where

$$\begin{aligned} 2H_g &= \frac{J_g \cdot \Omega_{B,g}^2}{2M_{B,g}} \cdot \omega_g \approx \frac{J_g \cdot \Omega_{B,g}^2}{2M_{B,g}} \\ D_g &= \frac{K_{Dg} \cdot \Omega_{B,g}^2}{M_{B,g}} \cdot \omega_g \approx \frac{K_{Dg} \cdot \Omega_{B,g}^2}{M_{B,g}} \end{aligned} \tag{4}$$

D_g is damping coefficient in *per unit*, which in this simplified expression represents the impact of damper windings, power system stabilizers, etc. Note that whereas the moment of inertia J_g is constant, H_g is only approximately constant (when ω_g is close to unity). Under small variations, the rotor dynamics can be written as follows:

$$2H_g \cdot \frac{d\Delta\omega_g}{dt} = \Delta p_{mg} - \Delta p_{eg} - D_g \cdot \Delta\omega_g \tag{5}$$

or in the complex domain by applying the Laplace transform:

$$2H_g \cdot s \cdot \Delta\omega_g(s) = \Delta p_{mg}(s) - \Delta p_{eg}(s) - D_g \cdot \Delta\omega_g(s) \rightarrow \Delta\omega_g(s) = \frac{\Delta p_{mg}(s) - \Delta p_{eg}(s)}{2H_g \cdot s + D_g} \tag{6}$$

By defining $\Delta p_g = \Delta p_{mg} - \Delta p_{eg}$, the derivative of the generator speed is:

$$\Delta\dot{\omega}_g(s) = s \cdot \Delta\omega_g(s) = \frac{s \cdot \Delta p_g(s)}{2H_g \cdot s + D_g} \tag{7}$$

The initial derivative of the generator speed can be computed from the initial value theorem when applying a step response of size Δp_d and computing the derivative of the speed variation or, being equivalent, an impulse of Δp_d and computing speed variation:

$$\begin{aligned} \Delta\dot{\omega}_g(t=0) &= \lim_{s\to\infty} s\left(s \cdot \Delta\omega_g(s)\right) \\ &= \lim_{s\to\infty} \frac{s \cdot \Delta p_g(s)}{2 \cdot H_g \cdot s + D_g} \cdot s \\ &= \lim_{s\to\infty} \frac{s \cdot \Delta p_d / s}{2 \cdot H_g \cdot s + D_g} \cdot s \\ &= \frac{\Delta p_d}{2 \cdot H_g} \end{aligned} \tag{8}$$

The relation between initial generator speed variation and an impulse is used in (Tuttelberg et al. 2018) for inertia estimation.

2.2 System inertia

In the past, system inertia was dominated by the sum of the inertia values of the large generating units. The total inertia of synchronous generators is computed as the sum of individual generator inertia values expressed on a common system rating, $S_{B,g}$:

$$H_{sg} = \sum_{g \in SG} \frac{H_g \cdot M_{B,g}}{S_{Bsg}} \tag{9}$$

where the system rating is defined as the sum of the ratings of the synchronous generators:

$$S_{Bsg} = \sum_{g \in SG} M_{B,g} \tag{10}$$

For low non-synchronous penetration levels, a linear relationship between system inertia and system demand has been assumed (Ashton et al. 2015). The more demand, the more synchronous generation units online; however, varying generation mixes involving different generation technologies could lead to different system inertias since individual inertia values depend on the generation technology. For high non-synchronous penetration levels, a (negative) correlation between the non-synchronous penetration level and the system inertia can be assumed (Du and Matevosyan 2018) (Allella et al. 2020). In this case, system inertia is computed by considering additionally non-synchronous generation capacity as follows:

$$H_{sys} = \sum_{g \in SG} \frac{H_g \cdot M_{B,g}}{S_{Bsg} + S_{Bnsg}} = \frac{H_{sg}}{1 + \frac{S_{Bnsg}}{S_{Bsg}}} \underset{\frac{S_{Bnsg}}{S_{Bsg}} < 1}{\approx} H_{sg} \cdot \left(1 - \frac{S_{Bnsg}}{S_{Bsg}}\right) \tag{11}$$

with the total rating of the non-synchronous generation being:

$$S_{Bnsg} = \sum_{g \in nSG} M_{B,g} \tag{12}$$

In order to consider further elements that provide direct (e.g., inertia emulation) or indirect (e.g., voltage-dependency of loads) inertial response, (Tuttelberg et al. 2018) defines the effective inertia. Indeed, (KUIVANIEMI M. et al. 2015) has shown that voltage-dependent load variations are dominant at the beginning of the disturbance, and thus affect inertia estimation. Effective inertia defines the relationship between a change in the power balance of the system or area and the rate of change of frequency of that area. In (Wilson et al. 2019), a quasi linear relationship between effective inertia, demand and total synchronous inertia of an area in UK has been found. In this line, (Phurailatpam et al. 2021) differentiates between synchronous and non-synchronous inertia. To include for instance non-synchronous generation that provides virtual inertia, the system inertia can be computed as:

$$H_{sys} = \sum_{g \in SG \cup g \in nSGv} \frac{H_g \cdot M_{B,g}}{S_{Bsg} + S_{Bnsg}} \tag{13}$$

2.3 Center of inertia

From the system point of view, a very useful quantity is the frequency of the center of inertia (COI), ω_{COI}:

$$\omega_{COI} = \frac{\sum_g H_g \cdot M_{B,g} \cdot \omega_g}{\sum_g H_g \cdot M_{B,g}} \tag{14}$$

The COI frequency is the inertia-weighted frequency (speed) of the generation units and its first derivative together with the knowledge of the system inertia makes it possible to estimate the initial active power unbalance. The COI frequency represents the system frequency by neglecting inter-machine oscillations. Indeed, generator and bus frequencies can be seen as variations around the COI frequency. If individual rotor dynamics are summed up and if we assume a uniform frequency ω:

$$\underbrace{\frac{2}{S_{Bsg}} \sum_g H_g \cdot M_{B,g}}_{=2H_{sg}} \cdot \frac{d\Delta\omega}{dt} = \sum_g \Delta p_{mg} - \sum_g \Delta p_{eg} - \sum_g D_g \cdot \Delta\omega \tag{15}$$

(Azizi et al. 2020) proposes a method to estimate the COI frequency by local measurements only. Inflection points of the local frequency (i.e., the instant when second time derivative of the frequency is cero) coincide with the COI frequency and the interpolation of the inflection points provides an estimate of the COI frequency. Filtering is needed.

2.4 Emulated or virtual inertia

Non-synchronous generation is able to provide inertia or rather an inertial response if appropriate controls are available. The control depends on the technology behind the non-synchronous generation as well as on the operation mode of the inverter. Wind generation involving rotating machines can provide inertial response by extracting kinetic energy from the rotor's inertia or by holding back power and activate this reserve if needed. Since PV generation or battery energy storage systems (BESSs) do not involve rotating masses, they can only provide inertial response by holding back power before activating it.

The grid-side inverters can be operated in grid-following or grid-forming mode. The control of grid-following inverters ensures the injection of given active and reactive powers by synchronizing the inverter and its controls with the grid, requiring the presence of a sufficiently strong grid and a PLL. Grid-forming inverters, by contrast can adjust, the imposed voltage and frequency as a function of the measured active and reactive power, for instance through droop controls, virtual synchronous machine implementation, etc. Grid-forming inverters are typically used for BESS, whereas grid-following inverters are used for PV generation.

Typically, grid-following inverters modify the active power set point by adding a frequency-variation-dependent signal, $\Delta p_{gfoll,ref}$:

$$\Delta p_{gfoll,ref} = \frac{b_1 \cdot s + b_0}{a_1 \cdot s + a_0} \cdot \Delta\omega_b(s) \tag{16}$$

where b_i, a_i are the parameters of the control transfer function, and $\Delta\omega_b$ is the bus frequency variation. Grid forming inverters can implement a series of power controllers. To some extent, these controllers are equivalent. To show the equivalence of droop control and virtual synchronous machine, let's formulate the droop control first:

$$\omega_{g,ref} = \omega_0 + m_p \cdot \left(p_0 - \frac{p_{eg}}{1 + s \cdot T_{fp}} \right) \tag{17}$$

where m_p is the droop constant, T_{fp} a time constant, p_0 the initial power set point, ω_0 the reference frequency, and p_{eg} is the converter's electrical power. By assuming constant power and frequency set points, p_0 and ω_0, this equation can be re-written as follows:

$$\omega_{g,ref} \cdot s \cdot \underbrace{\frac{T_{fp}}{m_p}}_{=2H} = p_0 - p_{eg} - \underbrace{\frac{1}{m_p}}_{D} \cdot \left(\omega_{g,ref} - \omega_0 \right) \tag{18}$$

Indeed, the dynamic equation relating the frequency generated by the grid-forming inverter and the power balance resembles the rotor dynamics of a synchronous generator.

3 Response phases to active power unbalances

Inertia estimation methods exploit different physical phenomena occurring just after an active power unbalance. The response of a power system to an active power unbalance during the first few seconds can be separated into several phases[3]:

- Rotor oscillations, depending on the electrical distance to the disturbance
- Rotor speed acceleration, depending on the disturbance and the inertia
- Primary frequency control, depending on the time constants (technology) and droops

Figure 1 illustrates the responses of the rotor speeds of two generators to an active power unbalance. Indeed, oscillations between rotor speeds can be observed. Whereas small disturbances basically lead to rotor oscillations, large disturbances lead to both rotor oscillations superimposing rotor speed acceleration. After some time, oscillations damp out and frequency is uniform.

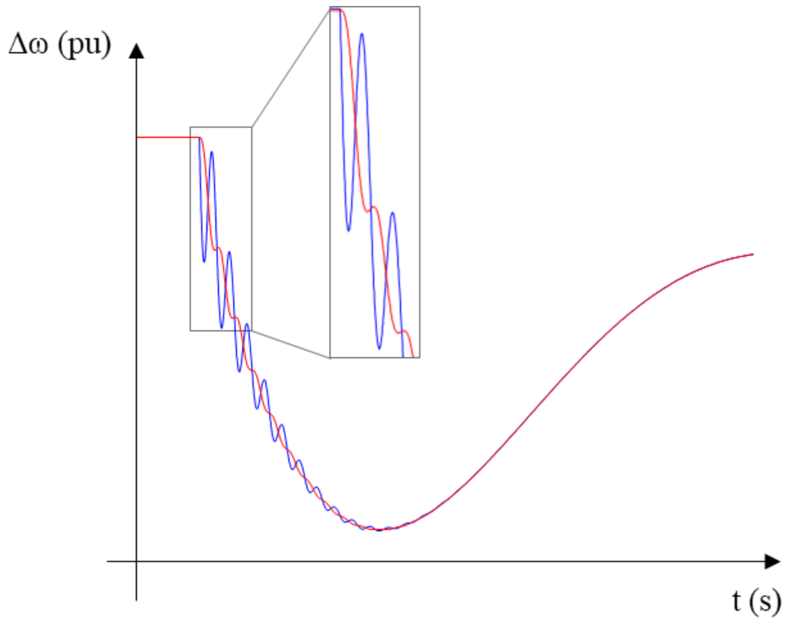

Figure 1: Illustration of the response of rotor speeds to an active power unbalance.

In general, the estimation methods make use of the first two phases to derive system inertia. Inertia affects the oscillation frequency of the electromechanical mode, i.e., the relative rotor speed oscillations. Inertia also affects the rotor speed acceleration. Usually, rotor speed acceleration has been assumed to be uniform, which is true in steady state but not during the transient, since persistence of oscillations depends on their damping.

[3] (Vorobev et al., 2019) presents approach to studying the long-term frequency distribution in power systems. A dynamic model with stochastic perturbations is used to derive an equation for the frequency deviations probability density function (PDF). System inertia has little effect on the frequency PDF, but aggregate system droop and deadband width have a major influence on the average frequency deviations.

3.1 Two-generator system

For the first two phases, a simple system consisting of two generators feeding a constant power load can be considered, illustrating the dominant factors.

3.1.1 Power sharing according to the electrical distance to the disturbance

Figure 2 shows the single line diagram of a two-generator system feeding an active power load and its equivalent circuit.

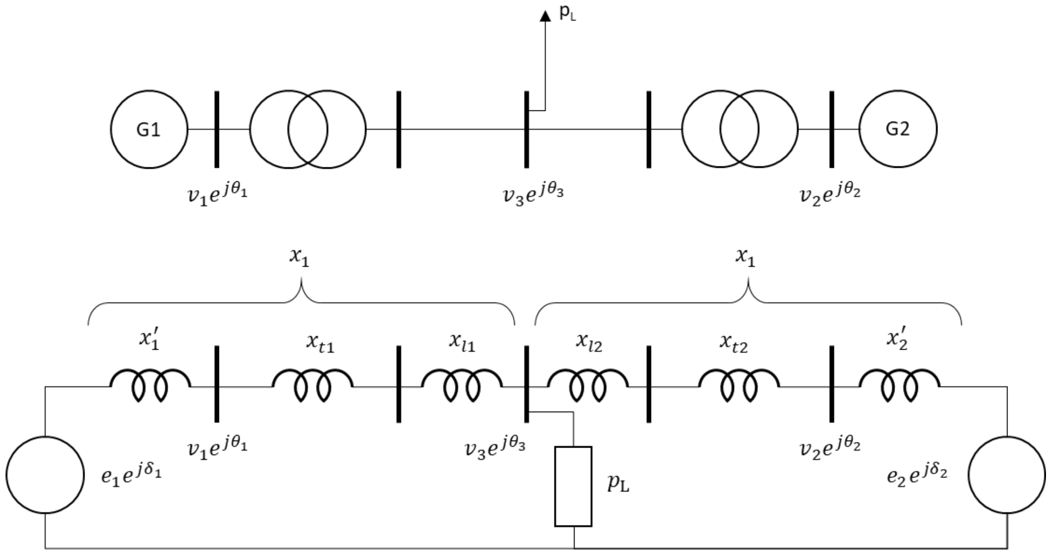

Figure 2: Single line diagram of a two-generator system feeding a load and its equivalent circuit.

The power balance in *per unit* at the load can be written as follows:

$$\begin{aligned} p_L &= p_{e1} + p_{e2} \\ &= \frac{e_1 \cdot v_3}{x_1} \cdot \sin(\delta_1 - \theta_3) + \frac{e_2 \cdot v_3}{x_2} \cdot \sin(\delta_2 - \theta_3) \end{aligned} \tag{19}$$

where p_L, p_{e1}, and p_{e2}, are the load power and generated powers, respectively, e_1, e_2, and v_3 are the voltage magnitudes, δ_1, δ_2, and θ_3 are internal and bus voltage angles, and x_1 and x_2 are the equivalent reactances. By assuming constant voltages, the variation of the power balance around an operation point results in:

$$\Delta p_L = \underbrace{\frac{e_{10} \cdot v_{30}}{x_1} \cdot \cos(\delta_{10} - \theta_{30})}_{p_{e10}} \cdot (\Delta\delta_1 - \Delta\theta_3) + \underbrace{\frac{e_{20} \cdot v_{30}}{x_2} \cdot \cos(\delta_{20} - \theta_{30})}_{p_{e10}} \cdot (\Delta\delta_2 - \Delta\theta_3) \tag{20}$$

This is similar to the DC power flow formulation. The variation of the angle of the load can be expressed in terms of the variations of the internal angles of the generators.

$$\Delta\theta_3 = \frac{p_{e10} \cdot \Delta\delta_1 + p_{e20} \cdot \Delta\delta_2 - \Delta p_L}{p_{e10} + p_{e20}} \tag{21}$$

If initial angle differences are small due to a change in the load and voltages magnitudes are constant and about equal ($e_{10} \approx e_{20} \approx v_{30} \approx 1$ pu), the power variation of generator 1 can be computed as follows:

$$\Delta p_{e1} = \frac{\Delta\delta_1}{x_1 + x_2} - \frac{\Delta\delta_2}{x_1 + x_2} - \frac{x_2 \cdot \Delta p_L}{x_1 + x_2} \tag{22}$$

In other words, if $x_1 \approx x_2$, and since internal angles cannot change suddenly, then generator g_1 picks up half of the load variation. If $x_1 << x_2$, then generator g_1 picks up most of the load variation. Congruently, the electrical distance to the perturbation initially determines the power picked up and larger speed oscillations could be expected at the generating unit with larger load variation pick up.

3.1.2 Rotor speed oscillations

The oscillations can be analyzed by means of the dynamic equations of the rotor. Instead of analyzing the individual speeds, the difference between speeds are studied, which describes the oscillations between them. In particular, the imaginary part of the complex eigenvalue of the dynamic system relates to the oscillation frequency. The dynamic equations are:

$$\begin{aligned}
2H_1 \cdot \frac{d\omega_1}{dt} &= p_{m1} - p_{e1} - D_1 \cdot (\omega_1 - 1) \\
\frac{d\delta_1}{dt} &= \Omega_0 \cdot (\omega_1 - 1) \\
2H_2 \cdot \frac{d\omega_2}{dt} &= p_{m2} - p_{e2} - D_2 \cdot (\omega_2 - 1) \\
\frac{d\delta_2}{dt} &= \Omega_0 \cdot (\omega_2 - 1)
\end{aligned} \tag{23}$$

For small variations,

$$\begin{aligned}
2H_1 \cdot \frac{d\Delta\omega_1}{dt} &= \Delta p_{m1} - p_{e10} \cdot (\Delta\delta_1 - \Delta\theta_3) - D_1 \cdot \Delta\omega_1 \\
\frac{d\Delta\delta_1}{dt} &= \Omega_0 \cdot \Delta\omega_1 \\
2H_2 \cdot \frac{d\Delta\omega_2}{dt} &= \Delta p_{m2} - p_{e20} \cdot (\Delta\delta_2 - \Delta\theta_3) - D_2 \cdot \Delta\omega_2 \\
\frac{d\Delta\delta_2}{dt} &= \Omega_0 \cdot \Delta\omega_2
\end{aligned} \tag{24}$$

By knowing that $\Delta p_L = \Delta p_{e1} + \Delta p_{e2}$ and defining and imposing that $K_{HD} = H_2 \cdot D_1 = H_1 \cdot D_2$, then the speed ($\Delta\omega = \Delta\omega_1 - \Delta\omega_2$) and angle ($\Delta\delta = \Delta\delta_1 - \Delta\delta_2$) differences can be written as:

$$\begin{aligned}
2H_1H_2 \frac{d\Delta\omega}{dt} &= H_2 \cdot \Delta p_{m1} - H_1 \cdot \Delta p_{m2} - (H_1 + H_2) \cdot p_{e10} \cdot (\Delta\delta_1 - \Delta\theta_3) + H_1 \cdot \Delta p_L - K_{HD} \cdot \Delta\omega \\
\frac{d\Delta\delta}{dt} &= \Omega_0 \cdot \Delta\omega
\end{aligned} \tag{25}$$

and by using the expression for voltage angle θ_3:

$$\frac{d\Delta\omega}{dt} = -\frac{K_{HD}}{2H_1H_2}\cdot\Delta\omega - \frac{H_1+H_2}{2H_1H_2}\cdot\frac{p_{e10}\cdot p_{e20}}{p_{e10}+p_{e20}}\Delta\delta\ldots$$
$$+\frac{H_2}{2H_1H_2}\cdot\Delta p_{m1} - \frac{H_1}{2H_1H_2}\cdot\Delta p_{m2} + \left(\frac{H_1}{2H_1H_2} - \frac{p_{e10}}{p_{e10}+p_{e20}}\cdot\frac{H_1+H_2}{2H_1H_2}\right)\cdot\Delta p_L \quad (26)$$
$$\frac{d\Delta\delta}{dt} = \Omega_0\cdot\Delta\omega$$

or written in matrix form by assuming constant mechanical power and considering load variation as the input variable:

$$\frac{d}{dt}\begin{bmatrix}\Delta\omega\\ \Delta\delta\end{bmatrix} = \begin{bmatrix}-\frac{K_{HD}}{2H_1H_2} & -\frac{H_1+H_2}{2H_1H_2}\cdot\frac{p_{e10}\cdot p_{e20}}{p_{e10}+p_{e20}}\\ \Omega_0 & 0\end{bmatrix}\begin{bmatrix}\Delta\omega\\ \Delta\delta\end{bmatrix} + \begin{bmatrix}\frac{H_1}{2H_1H_2} - \frac{p_{e10}}{p_{e10}+p_{e20}}\cdot\frac{H_1+H_2}{2H_1H_2}\\ 0\end{bmatrix}\Delta p_L \quad (27)$$

The oscillation frequency is related to the imaginary part of the complex eigenvalues:

$$\lambda_{1,2} = -\zeta\cdot\omega_n \pm j\omega_n\sqrt{1-\zeta^2} \quad (28)$$

Where

$$\omega_n = \sqrt{\Omega_0\frac{H_1+H_2}{2H_1H_2}\cdot\frac{p_{e10}\cdot p_{e20}}{p_{e10}+p_{e20}}}$$
$$\zeta = \frac{1}{2}\frac{K_{HD}}{2H_1H_2}\frac{1}{\omega_n} \quad (29)$$

The eigenvalues indicate a damped oscillatory response. Figure 3 illustrates the damped oscillatory response of the speed difference between generator 1 and generator 2. Since rotor speeds in steady state are equal, the speed difference in steady state tends towards zero.

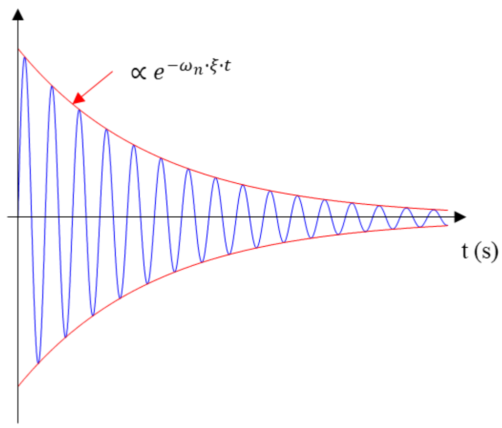

Figure 3: Illustration of a damped oscillatory response of the speed difference.

In the absence of damping sources such as damper windings, power system stabilizer, etc. (i.e., $K_{HD} = 0$), the oscillation frequency is equal to the natural frequency ω_n and depends only on the inertia relation and on the initial power point relation (or approximately, on the respective electrical distances). The instant, t, where the oscillation amplitude falls below a certain threshold, A, can be computed as:

$$t = \frac{\ln(A)}{-\zeta \cdot \omega_n} \tag{30}$$

For instance, with $H_i = 4$, $D_i = 20$, $P_{ei0} = 5$, and $A = 0.1$, $t = 1.84$ s. In other words, and depending on the damping coefficient, oscillations are well damped out between 1.5 to 3.5 s.

3.1.3 Rotor speed acceleration

Due to the power unbalance caused by the load variation, the rotor starts slowing down. Rotor oscillations analyzed previously are superposed to this deceleration. If the oscillations are sufficiently well damped after the first few instants, one can assume that frequency and its ROCOF vary about uniformly throughout the system.

$$\frac{d\Delta\omega_1}{dt} \approx \frac{d\Delta\omega_2}{dt} = \alpha \tag{31}$$

By neglecting the damping coefficient D, the following relation can be found:

$$\frac{\Delta p_1}{2H_1} \approx \frac{\Delta p_2}{2H_2} = \alpha \tag{32}$$

The inertia of each generator can thus be estimated if the power variations at each generator terminal can be measured and by assuming a uniform ROCOF. Indeed, for a given (known) system power unbalance, the system inertia can be estimated as:

$$\frac{\Delta p_L}{2\alpha H_1} \approx (H_1 + H_2) \tag{33}$$

3.2 Large systems

For large systems, network equations including the transient reactance of generators can be written as follows when making use of the DC power flow formulation:

$$\begin{bmatrix} \Delta\mathbf{p}_G \\ \Delta\mathbf{p}_L \end{bmatrix} = \begin{bmatrix} \mathbf{A}_1 & \mathbf{A}_2 \\ \mathbf{A}_3 & \mathbf{A}_4 \end{bmatrix} \cdot \begin{bmatrix} \Delta\boldsymbol{\delta}_G \\ \Delta\boldsymbol{\theta}_L \end{bmatrix} \rightarrow \Delta\mathbf{p}_G = \underbrace{\left(\mathbf{A}_1 - \mathbf{A}_2 \cdot \mathbf{A}_4^{-1} \cdot \mathbf{A}_3\right)}_{=\mathbf{L}} \cdot \Delta\boldsymbol{\delta}_G + \mathbf{A}_2 \cdot \mathbf{A}_4^{-1} \cdot \Delta\mathbf{p}_L \tag{34}$$

Since initially the internal angles cannot vary, load variations translate into generator power variations according to electrical distance contained in matrices $\mathbf{A}_2$ and $\mathbf{A}_4$. Apart from this conclusion, equation (34) shows that, under constant load ($\Delta\mathbf{p}_L = 0$, being true for buses without connected loads), load and internal voltage angles are related, i.e., load frequencies are imposed by generator speeds[4].

The dynamic equations become:

$$\begin{bmatrix} \dfrac{d\Delta\boldsymbol{\omega}}{dt} \\ \dfrac{d\Delta\boldsymbol{\delta}_G}{dt} \end{bmatrix} = \begin{bmatrix} -\dfrac{1}{2}\cdot\mathbf{H}^{-1}\cdot\mathbf{D} & -\dfrac{1}{2}\cdot\mathbf{H}^{-1}\cdot\mathbf{L} \\ \Omega_0\cdot\mathbf{I} & \mathbf{0} \end{bmatrix}\cdot\begin{bmatrix} \Delta\boldsymbol{\omega} \\ \Delta\boldsymbol{\delta}_G \end{bmatrix} + \begin{bmatrix} \dfrac{1}{2}\cdot\mathbf{H}^{-1}\cdot\mathbf{A}_2\cdot\mathbf{A}_4^{-1} \\ \mathbf{0} \end{bmatrix}\cdot\Delta\mathbf{p}_{\mathbf{L}} \tag{35}$$

where **L** is a matrix describing the network relation, and **H** and **D** are diagonal matrices containing the inertia values and damping coefficients, respectively. Modal analysis can be applied to evaluate eigenvalues, eigenvectors and participation factors, numerically. If **D** is neglected:

$$\frac{d^2\Delta\boldsymbol{\delta}_G}{dt^2} = \underbrace{-\frac{1}{2}\cdot\Omega_0\cdot\mathbf{H}^{-1}\cdot\mathbf{L}}_{\mathbf{A}_{sys}}\cdot\Delta\boldsymbol{\delta}_G \tag{36}$$

Along this line, (Pagnier and Jacquod 2019) further represents the Laplacian in terms of its eigenvalue matrix and the right eigenvector matrix:

$$\mathbf{L} = \mathbf{V}\cdot\boldsymbol{\Lambda}_L\cdot\mathbf{V}^{-1} \tag{37}$$

and the eigenvalue of the system (of $\mathbf{A}_{sys}$) can be related to the eigenvalues of the network Laplacian. If all inertia values were the same and equal to H (**H** = **I**/2/H, where **I** is the identity matrix), the system matrix $\mathbf{A}_{sys}$ becomes:

$$\mathbf{A}_{sys} = \frac{1}{2}\cdot\Omega_0\cdot\mathbf{H}^{-1}\cdot\mathbf{V}\cdot\boldsymbol{\Lambda}_L\cdot\mathbf{V}^{-1} = \mathbf{V}\cdot\frac{\mathbf{I}\cdot\Omega_0\cdot\boldsymbol{\Lambda}_L}{2H}\cdot\mathbf{V}^{-1} \tag{38}$$

Indeed network Laplacian eigenvalues are modified by a factor inversely proportional to the inertia. In other words, the network plays a significant role in the oscillations. When analyzing the impact of inertia distribution on the disturbance propagation of a simplified model of the continental European system (by considering lossless network, classical generator model, frequency-dependent loads), (Pagnier and Jacquod 2019) shows that disturbance propagation is not only governed by the inertia distribution, but also by its location, i.e., the electrical distance, which is taken into account by contemplating the eigenvalues of the network

[4] This has been shown in a more systematic way by the frequency divider in (Federico Milano & Alvaro Ortega Manjavacas, 2020a).

Laplacian. In particular, the slowest mode, called Fiedler mode, has a large impact, and adding inertial response in Fiedler areas (areas participating in the Fiedler mode) is beneficial.

4 Review

4.1 Overview

Inertia estimation is a parameter estimation problem. In power systems, static and dynamic state estimation are differentiated. (Zhao et al. 2021) provides a comprehensive clarification of the roles of the dynamic state estimation (DSE) from the power system modeling, monitoring, and operation perspectives. Measurement configurations, model requirements, software support and potential applications are discussed. Among others, DSE applications include generator inertia and reactance estimation, estimation of frequency and ROCOF of the COI, frequency stability assessment, etc. (Kryonidis et al. 2021) gives a brief review on inertia estimation. Further, modal identification and equivalent modeling of distribution networks is reviewed. Indeed, inertia estimation and its distribution in distribution systems can also be understood within equivalent modeling and identification of distribution systems. Nonetheless, equivalent models are usually developed from the TSO perspective at the point of connection (POC), yielding to single inertia value offered by the distribution system but without providing a distribution of the inertia. (Heylen, Teng, and Strbac 2021) discusses challenges and opportunities of inertia estimation and forecasting in low-inertia power system. Operation constraints and measures to tackle reduced inertia levels have been reviewed, with a particular focus on UK and the Nordic systems.

4.1.1 Trigger and execution time

(Cai et al. 2019) differentiates between static and dynamic approaches. In static calculations, system inertia equals the weighted average of the inertia values of the generators at the same capacity. To overcome the shortcomings of static approaches (lack of data of distributed generation (DG), insensitivity to inertia changes) estimation methods that use recorded system responses have been developed. Such dynamic approaches can be further classified in the way measurements are obtained: event-based estimation and continuous estimation. Measurement data used can be usually divided into three types (Guo, Norris, and Bialek 2014):

- ringdown signal (disturbances),
- ambient signal (continuous small disturbances),
- and probing (injection) signal.

Ringdown signals normally occur after large system disturbances, while ambient signals are present when the system is subject to continuous small disturbances such as load variations. Probing signals are procured testing pseudo-random noise is injected intentionally.

Measurements can be either extracted from DFR or PMUs. Whereas DFR can capture electromagnetic transients, PMUs can measure electromechanical transients (Fan, L., Miao, and Wehbe 2013). The available data from DFR are stator phase currents and voltages at the terminals of synchronous machines, and the field voltage and current. Available data from PMUs consists of voltages, voltage phase angles, and real and reactive power.

(Heylen, Teng, and Strbac 2021) further divides inertia estimation methods into offline, online and forecast methods according to the execution instant and estimation horizon. Forecast methods, as classified by (Heylen, Teng, and Strbac 2021), are however mostly online methods, estimating the inertia with different time resolutions. Indeed, some online methods estimate the currently available inertia (real time), whereas others estimate the inertia with lower time resolution (e.g., for the current hour) but also could estimate inertia larger time horizons (e.g., several hours or the next day).

4.1.2 Underlying physical concept and evaluation method

Estimation approaches can also be differentiated according to the evaluation method and the underlying physical concept:

- Electromechanical modes
- Frequency (speed) acceleration (swing equation)

Estimation approaches based on oscillation modes employ different mode identification methods, which also depend on the way the measurements have been obtained (Guo, Norris, and Bialek 2014). Prony analysis uses ringdown signals following a large disturbance, whereas Wiener-Hopf equations, recursive methods, or empirical mode decomposition can be used for ambient signals. Estimation methods based on the swing equation use different degrees of modeling details, from neglecting the equivalent damping term, over including other frequency and voltage-dependent terms, to explicitly contemplating the lost inertia after a generation outage. The computation of the inertia making use of the swing equation differently evaluates the angle, frequency and power derivatives by means of polynomial approximations, finite differences, sliding windows, moving average windows, etc. (Heylen, Teng, and Strbac 2021) differentiated the methods according to the domain of the underlying models: time-series models, models in the Laplace domain, and models in the modal domain. Indeed, many methods starting from the swing equation use time-series and Laplace-domain models.

4.2 Classification

This section reviews and classifies the state of the art of inertia estimation according to the scope, the methods, and whether the focus lies on the amount of inertia or its distribution. Although inertia estimation is a model identification problem and the estimation of the inertia as such is a result of model identification, particular attention is paid on literature explicitly tackling inertia estimation.

4.2.1 Scope

Inertia estimation approaches can be differentiated according to their scope. The scope of the methods are: system-wide, area-wide, element-wise.

4.2.1.1 System-wide

Most of the approaches aim at estimating system inertia. In many cases, they use a frequency measurement at a single location by assuming that the measurement location coincides with the COI tacitly (see (Inoue et al. 1997), (Wall and Terzija 2014), etc.) and by estimating or assuming the active power unbalance. Other approaches approximate the COI frequency by using several frequency measurements and computing the average (Schiffer, Aristidou, and

Ortega 2019), an inertia weighted average (Zografos, Ghandhari, and Eriksson 2018a), (Azizipanah-Abarghooee et al. 2019), etc.

Modal information can also be used to estimate system inertia. If the n-1 independent electromechanical modes of a n-machine power system were measurable, only n-1 inertia values could be estimated (Guo, Norris, and Bialek 2014). System inertia is then computed by summing up individual inertia values. For larger (multi-area) systems (Cai et al. 2019) builds a two-area equivalent, where the challenges reside in identifying the equivalent two-area system and reducing the initial system to the two-area one. (Yang et al. 2020) also proposes a method for identifying and building a two-generator equivalent of an interconnected power system for a particular mode.

(Best, Brogan, and Morrow 2021) estimates the system inertia by making use of known perturbations, caused by the flow changes on a HVDC interconnector. Similarly, (S. Shah and V. Gevorgian 2019) proposes a system inertia estimation making use of a frequency response function between a known active power injection and the measured frequency at the point of injection.

(A. Schmitt and B. Lee 2017) describes the use of an artificial neural network (ANN) to estimate system, area and bus inertia under normal operation conditions. Whereas area and system inertia could be predicted relatively well, bus inertia prediction is far less accurate since the relation between modal information and individual bus inertias is less clear. A similar approach has been persued by (E. S. N. R. Paidi et al. 2020) .

(X. Cao et al. 2016) presents a switching Markow Gaussian model (SMGM) to estimate system inertia online during normal operation conditions. (Allella et al. 2020) proposes a method which uses a stochastic process to estimate the system inertia.

4.2.1.2 Area-wide and regional

The estimation of area-wide and regional inertia has also been treated in the literature. System inertia can then be computed by summing up the inertia of the areas. (Tuttelberg et al. 2018) presents a method where system inertia is obtained from the set of individual area inertia values, with the boundaries of each area previously defined. Similarly, (Ashton et al. 2015) compute the total system inertia by summing up regional inertia values of large synchronous generators, assumed being known. (Wilson et al. 2019) also assumes that the power system can be considered as multiple centers of inertia, coupled through the network. (G. Chavan et al. 2017) defines the area equivalents by using historical coherency and the pilot bus of each equivalent area needs to be equipped with a PMU for inertia estimation. (Cai et al. 2019) obtains its two-area equivalent by an appropriate network reduction including coherency.

(Guo, Norris, and Bialek 2014) estimates inertia of synchronous generators by employing modal information extracted from online WAMS measurements. (Panda, Mohapatra, and Srivastava 2020) describes another online method to estimate element and area inertia to a known or detected disturbance. Modal information is extracted by using ESPRIT. Similarly, (Yang et al. 2021) presents a disturbance-based estimation of area effective inertia by extracting inter-area modal information from PMU measurements by means of DMD.

Other area or rather regional inertia estimation methods have also been proposed. (Fan, Miao, and Wehbe 2013) presents a method based on PMU measurements, estimating the inertia downstream of the measurement location. Similarly, (Lugnani et al. 2020) describes a disturbance-based inertia estimation approach of a single or a group of generators. Inertia of generators downstream of the location of the PMU measurement can be identified. (Liu, Chen, and Milano 2021) makes use of the rate of change of power (ROCOP) to estimate the inertia of a synchronous or non-synchronous or a group of generators.

(Zeng, Zhang, Zhou et al. 2020) estimates bus inertia from ambient data. (Zeng, Zhang, Chen et al. 2020) extends the approach proposed in (Zeng et al. 2020). Electrical power and frequency at each generator bus or at area or system-level need to be measured by PMUs.

4.2.1.3 Element-wise and local

Significant effort has been devoted to synchronous machine model validation and parameter calibration, involving among others the inertia parameter. Parameter calibration of synchronous machines can be traditionally implemented using staged tests, conventional online tests, or PMU-based tests (Z. Huang et al. 2013).

Method	Point in time	Online/offline	Data
Staged test	Commission or scheduled	Offline	Standstill frequency response
Conventional online test	Scheduled, set point variations, or disturbances	Online	Large/small disturbance response
PMU-based test	Ambient or Disturbance	Online	Large/small disturbance response

Table 1: Parameter identification methods of synchronous machines (Z. Huang et al. 2013).

(Z. Huang et al. 2013) proposes an online parameter estimation method of synchronous machine by using enhanced Kalman filter (EKF) and PMU measurements, that are played-back5 to a suitable 4th-order model to estimate the inertia, the exciter and the PSS gain. These parameters have been selected by correlating the frequency spectrum of the measured active and reactive powers with the spectrum of the trajectory sensitivities of all parameters. (Fan, Lingling and Wehbe 2013) uses a similar approach but by employing an iterative EKF, which improves convergence of the Kalman filter process but at a higher computation cost. Unscented Kalman filter (UKF) and a modified Kalman filter have been used to estimated, among others, the inertia value of individual generators in (Ariff, Pal, and Singh 2015) and (Zhao, Tang, and Terzija 2019), respectively.

(Wang, B. et al. 2020) describes an online inertia estimation algorithm that makes use of ambient data to extract modal information on the electromechanical oscillations. With respect to inertia

[5] Two play-back methods have been reported. Method A applies measure voltage and frequency signal to the model and the resulting active and reactive powers are compared with the measured ones. Method B applies active and reactive powers to the model and compares the measured and obtained voltage and frequency (Fan, Lingling & Wehbe, 2013).

estimation, (Sun, M. et al. 2019) presents an online inertia estimation algorithm making use of PMU measurements obtained at the terminals of every generator, measuring power and frequency to compute ROCOF and inertia. (Liu, Chen, and Milano 2021) makes use of the rate of change of power (ROCOP) to estimate the inertia of a synchronous generators. (Tavakoli et al. 2012) proposes a grey-box approaches to estimate generator inertia by making use of a standard dynamic model of the governor and including the inertial response (swing equation) and by minimizing the difference of the measured and simulated energy responses, weighted exponentially in time to compensate for the governor response. The impact of sampling rate, time shift and moving average filter window length have been studied, and results show that the window length of the filter has most impact and that sampling frequency should be at least 8 Hz.

Inertial response of RES has also been analyzed and identified. Indeed, (He, Yuan, and Hu 2017) shows that the inertial response of a DFIG depends on the PLL and the active power control loop. A synthetic internal voltage, similar to the one of the classical synchronous machine model, is derived, and the dynamics of its associated angle are affected by the PLL and the active power control loop. As a result, the inertia can be changed by tuning the parameters of the PLL. The transfer function indicates that the inertia will decrease during a dynamic process. A fast PLL results in a fast angle movement, and thus an effective low inertia, whereas a slow PLL results in an effective high inertia. In this regard, the absence of the PLL (and controls) would result in trespassing the natural inertia of the DFIG. (Beltran et al. 2018) estimate the emulated inertia of wind farms. The method assumes that the inertia emulation resembles a virtual swing equation. The swing equation is expressed in terms of the bus voltage angle obtained by PMUs and discretized through a 4th-order central finite-difference scheme. The estimation requires detecting the beginning of the disturbance, the peak value of the first angular oscillations, and knowing the active power produced by the wind farm. (Lu et al. 2020) considers and builds a mixed copula-based conditional probability distribution model of the wind speed, considering wake effect, wind shear conditions, and time delay of wind speed. The available inertia is evaluated in terms of "available kinetic energy" and "available additional active power", which both depend on the condition probability distribution of the wind speed. This provides inertia bounds with a certain degree of confidence.

4.2.2 Inertia estimation methods

4.2.2.1 Dispatch status

Under the assumption that the commitment of all synchronous generators as well as their inertia constant is known, the system inertia can be estimated. Indeed, (W. Winter et al. 2015) mentions that the position of circuit breakers connecting synchronous generators to the power system has been investigated as a method for helping to determine the online inertia. Such an approach is currently used to monitor inertia in the Nordic countries (ENTSO-e 2018).

(Du and Matevosyan 2018) proposes monitoring ERCOT’s system inertia in MWs by making use of the generators’ current operation plan (COP) and by assuming known inertia constants of the generators. The COP submitted by each generator in ERCOT provides an estimate of unit status (on/ off) and operating limits for the next 168 hours. A three-hour ahead forecast of the system inertia seems to work well for evening hours with high prices (or in general, for high-inertia scenarios), whereas the error for morning hours with low prices (for low-inertia scenarios) is significant since generating units change their commitment status with respect to the COP. These errors require including additional bias to the forecast when low energy prices are likely to result in low inertia.

A drawback of such methods is that data for inertia constants in the TSO databases of the generators seem to be unreliable, and not all generators send their breaker positions to the SCADA system. This is an additional issue in case of small distributed generators.

4.2.2.2 Equivalent network modeling

The development of equivalent dynamic models of active distribution networks (ADN) (Glavic 2016). Growing TSO-DSO interactions further foster this research line.

(Yu, El-sharkawi, and Wvong 1979) proposes a simplified equivalent model to dynamically represent the large power system in the neighboring area of a local power system instead of an infinite bus approximation. The power system is represented by a linear model, whose parameters are estimated by using a least-square estimation algorithm, i.e., its inertia, damping coefficient, synchronous and transient reactance, and the field time constant. (X. Feng, Z. Lubosny, and J. Bialek 2006) propose a method to derive a dynamic equivalent of a distribution system. The distribution system is considered as a black-box, a model with unknown structure. Voltage and frequency were used as input, and real and reactive power as output. The election of suitable disturbances is discussed, and finally disconnection and re-connection of loads within the distribution system is proposed in order to excite as much as possible only the distribution system response. ARX and state-space models have been identified. A black-box approach does not allow for specific parameter estimation, e.g., the inertia. Results seem to depend much on the type and location of the disturbance. (J. V. Milanović and S. Mat Zali 2013) validate a grey-box model of a distribution system. The assumed equivalent model structure of ADN comprises a converter-connected synchronous generator in parallel with a composite load model. Converter-connected synchronous generation simplifies converter modeling. Current control dynamics are neglected. Similarly to (X. Feng, Z. Lubosny, and J. Bialek 2006) , real and reactive power at the connecting point are the outputs, and voltage and frequency at the connection point are the inputs to the equivalent model. (G. Chaspierre et al. 2020) also propose a grey-box model, where converter-connected generation and static and dynamic motor loads are electrically separated to consider their different location. Monte-Carlo simulations are used to consider uncertain parameters. A weighted least-square identification is used such that measured active and reactive power approaches their averages, weighted by the inverse of the variance. An experimental validation of a grey-box equivalent dynamic model for a microgrid is described in (F. Conte et al. 2021). The equivalent model includes synchronous machine, a ZIP load, and converter-connected elements, modelled as linear functions of the voltage and frequency deviation. A set of experimental tests have been successfully carried out on a real low voltage (LV) microgrid considering different configurations, including both grid-connected and islanded operating conditions, to show the effectiveness of the approach.

4.2.2.3 Model fitting and regression

Measurements of frequency and active power can be used to identify predefined models and their parameters. This identification can be carried-out online or offline. Sufficient disturbance must occur therefor. In most of the proposals, PMU measurements are needed. Most models are based on the swing equations, which in some cases is modified to consider frequency and/or voltage-dependency of loads, the loss of inertia corresponding to a generation outage, etc.

4.2.2.3.1 Frequency and ROCOF fitting

(Inoue et al. 1997) makes use of a 5th-order polynomial approximation with respect to time to approximate the response in terms of frequency of the system. Response to known disturbances are thus needed. A suitable disturbance event is detected if the absolute value of the ROCOF exceeds 0.04 Hz/s. Frequency, measured at various 500 kV substations or switching stations, is filtered by a moving average filter. This polynomial approximation with coefficients a_i filters the frequency oscillations (thus $\omega_g = \omega$) and system inertia is estimated as follows.

$$2H_{sys} = -\frac{\Delta p}{\left.\frac{d\omega}{dt}\right|_{t=t_0}} = -\frac{\Delta p}{a_1} \tag{39}$$

In (Tavakoli et al. 2012) a white-box approach is proposed to estimate system load inertia. Load inertia is deduced from the system inertia by subtracting the generator inertia and the inertia of type 1 and 2 wind generators[6]. System inertia is computed by using a polynomial like in (Inoue et al. 1997). Inertia of wind generators has been assumed to amount to 3 MWs/MVA. The inertia constants of generators are known in that approach.

(Phurailatpam et al. 2020) extends the approach in (Inoue et al. 1997) to microgrids with significant penetration of non-synchronous generation. In addition to the frequency curve fitting to determine system inertia, a curve fitting process is also applied to the power variations (to take into account other factors such as voltage-dependency of loads, etc.). Power is measured at every generating unit. The order of the polynomial of the frequency curve fitting is variable and depends on the estimation accuracy with respect to an inertia estimation making use of the maximum ROCOF. In case of high penetration of non-synchronous generation, the approach loses accuracy since inertia emulation is not instantaneous and thus different to inertial response of synchronous generation.

(Sun et al. 2019) presents an online inertia estimation algorithm making use of PMU measurements obtained at the terminals of every generator. PMUs measure electrical power and frequency. By knowing the variation of the electrical power and by computing the ROCOF, the inertia of every generator can be estimated by considering its connection status. Instead of using a polynomial approximation like in (Inoue et al. 1997), ROCOF itself is estimated by a linear frequency response model, consisting in a linear combination of average frequency and ROCOF multiplied by the sampling period. The ROCOF can be estimated by a least square method (Moore-Penrose inverse). A sufficiently large perturbation is needed.

(Zografos, Ghandhari, and Eriksson 2018) proposes a disturbance-based estimation of the system inertia. Unlike others, the proposed approach considers both frequency and voltage dynamics of the system, and in particular voltage and frequency-dependence of the load. Two

[6] In (Sigrist & Rouco, 2017) it has been shown that induction machine introduces a slightly delayed inertial response. This response depends on the inertia, the initial loading and the load type.

separate methods, which can be combined, modify the swing equation by including a frequency-dependent term (reflecting load variations, but also possible frequency controls) and/or a voltage-dependent term (reflecting load-voltage dependency). The disturbance is supposed to be known. Both methods need pre-defined, suitable post-disturbance instants to identify frequency and voltage dependency, whereas the frequency-dependent method in addition requires additional measurement samples to estimate the frequency dependency, augmenting the model. Voltage-dependent variation is derived by using the average generator voltages and a ZIP model, assuming some known parameters. Inertia-weighted generator frequencies and its derivative are used as input signal for the estimation. The combined method works best.

(Sun, Q., Li, and Philhower 2021) presents a disturbance-based system inertia estimation. The method makes use of the R-approach defined in (Zografos, Ghandhari, and Eriksson 2018b). Disturbance size needs to be known. Frequency and its derivative are filtered by means of median and moving average filters. A Gaussian progress regression method is used to predict the dynamic post-disturbance behavior of the system.

4.2.2.3.2 Transfer function

(Schiffer et al., 2019) uses the dynamic regressor and mixing (DREM) approach to estimate system inertia and total mechanical power set point of generating units under primary frequency control (PFC). The system inertia is estimated by using an equivalent swing equation and by measuring the frequencies and the electrical power of the generating units under PFC, as well as the total mechanical power of the generating units under PFC after disturbances (outages and re-scheduling). The total mechanical power under PFC can also be estimated by using suitable model and the average frequency. COI frequency is approximated by the average frequency, computed from the measured frequencies. Measurements are filtered and the equivalent swing equation is transformed into a standard regression form. Since two parameters need to be estimated but only one equation exists, the regression is augmented by a second, delayed equation. The gradient algorithm is then used to obtain parameter estimates. Delay, filter constant and two parameters of the gradient algorithm are needed. Time of convergence of the algorithm seems to be related to the system dynamics.

(Tuttelberg et al., 2018) presents a method to estimate system inertia from ambient measurements data of active power and frequency. System inertia is obtained from area inertia, with the boundaries of each area previously defined. The inertia of each area is estimated by observing the dynamics between changes in active power demand of the area and the resulting weighted-average frequency deviation of the area during normal operation of the system for two to six minutes. Load demand variations are deduced from inter-area flows and the area generation. An ARMAX model is identified, converted to a further reduced-order continuous time model, and the area inertia is identified by its impulse response (see equation (8)):

$$\begin{aligned} \dot{\omega}_g\left(t=0\right) &= \lim_{s\to\infty} \omega_g\left(s\right) \\ &= \lim_{s\to\infty} \frac{b_{n-1}\cdot s^{n-1}+\ldots+b_0}{a_n\cdot s^n+\ldots+a_0}\cdot 1\cdot s \\ &= \frac{b_{n-1}}{a_n} \end{aligned} \tag{40}$$

(Lugnani et al., 2020) describes a sliding-window disturbance-based inertia estimation approach. A second-order ARMAX model is used, and its parameters are identified by a one-step look ahead prediction error problem, solved by gradient-based optimization method. The method requires PMUs measurements, which are filtered by a Butterworth filter of 0.5 Hz and assumes that a known disturbance has been detected. The post-disturbance window length minimizes the estimation variance. The selected disturbance should not be too close to the PMU since it might corrupt measurements and differences between speed and bus frequency might be too high. Recording length is 30 s, with two cycles for pre-disturbance measurement and a few cycles for post-disturbance measurement, depending on the variance of the estimation. The identified discrete model is transformed into a continuous-time model as in (Tuttelberg et al., 2018).

(Kontis et al., 2021) compares two estimation methods quantitatively: a sliding-window-based approach ((Wall & Terzija, 2014)) and an ARMAX-based approach (see (Lugnani et al., 2020)). The impact of window length, noise level, disturbance magnitude and location as well as the RES penetration level is analyzed and compared. Monte Carlo simulations with an SFR model and with IEEE 9-bus system are run. Shorter window lengths are beneficial for disturbance-based estimations. It seems that ARMAX model works better under moderate noise levels, whereas it might fail to provide inertia estimations under high noise levels. For moderate levels, window lengths seem to be bounded. Whereas both methods work well under different disturbance magnitudes, the sliding-window-based approach seems to be more robust against varying disturbance locations and its window length is hardly influenced by the locations. RES penetration level does not practically affect the performance.

(Phurailatpam et al., 2021) describes a disturbance-based approach to estimate the non-synchronous inertia of AC microgrids. The approach is based on a low-order representation of the microgrid's frequency dynamics, like the SFR models used in the literature, where Diesel generators, BESS and other contributions to the inertial response and frequency control are modelled as linear transfer functions. The approach assumes that synchronous inertia of Diesel generators and the disturbance are known. If the active power output of the Diesel generator is known, the governor response can be estimated. According to the availability of the estimated governor response, a SISO or a MISO identification method is proposed to estimate no-synchronous inertia. Possible input and output non-linearities are considered a posteriori through Hammerstein-Wiener models, but whereas these models improve response accuracy, no conclusions on the estimation of the inertial response are deduced. The impact of load contribution (frequency and voltage dependency) has not been considered.

(Zeng et al., 2020) extends the approach proposed in (Zeng et al., 2020) (see section 4.2.3.2). Electrical power and frequency at each generator bus or at area or system-level need to be measured by PMUs. For area and system-wide estimation, weighted-average frequency is used with weights inversely proportional to frequency variance. Measurements are detrended and then filtered by a Butterworth filter of 0.5 Hz cut-off frequency. A general model of the generator, area or system and its most appropriate order are obtained by a subspace identification method for a given window length. The model is then excited by a unity step to obtain the ROCOF and lastly the inertia. The estimated inertia over a given window is updated with a given refresh rate using new estimations available. An exponential smoothing method is also used to further smooth inertia estimation.

4.2.2.4 Numerical evaluation of the swing equation

The swing equation can be used to estimate an equivalent inertia if frequency and active power measurements are available (see sections 2 and 3.1.3). ROCOF can then be numerically computed in different ways by using finite differences, sliding windows, etc. Such swing-equation-based methods can estimate the inertia offline or online in case of a sufficiently rich disturbance. In case of online estimation, the detection and identification of the disturbance is a key point.

(Chassin et al., 2005) estimates the system inertia from frequency measurements of a single location, with a resolution of 0.1 s and a 0.001 Hz after a suitable event. The measurements are filtered by a 0.5-Hz filter before estimating the inertia through the swing equation. From 167 events, a somewhat linear relationship between system demand and system inertia has been identified. Variations of inertia for a given system demand might be due to factors such as seasonal and diurnal variations of dispatch, annual variations of hydro generation and its available inertia, and variations of the actual lost power output with respect to the assumed (scheduled) output.

(Bian et al., 2018) proposes a method to determine inertia contribution of demand by estimating system inertia from past frequency events and subtracting the generation contribution from it. System inertia is computed from the known unbalance size and the ROCOF. The generation-side contribution is estimated from the dispatched power, corrected by a factor that relates power output to the capacity (this factor is the system primary frequency control gain by assuming that reserve is correlated with the capacity). The results indicate that on average 20% of the total system inertia was provided from the demand side with an average inertia of 1.75 s in 2010. Penetration of VFD motor loads will increase primary frequency control requirement.

(Ashton et al., 2015) proposes a method to estimate the total system inertia after suitable events. The method uses of PMU measurements. Frequency is calculated from time derivatives of voltage phasor angles and filtered by means of a Butterworth low pass filter of 0.5 Hz cut-off frequency to minimize the influence of the measured transients before estimating the RoCoF[7]. The suitability of an event is determined by a detrended fluctuation analysis (DFA), comparing fluctuations with a threshold. A suitable event is chosen when the fluctuation decreases below the threshold within 1 s. Total system inertia is finally deduced by summing up regional inertia values of large synchronous generators, assumed being known. This sum is multiplied by the real size of the disturbance and divided by the estimated size, obtained as the product of the regional frequency derivative computed over a 500 ms sliding window and the regional inertia. The paper shows that seven PMU measurements (seven regions) are sufficient to estimate the GB inertia and that the linear relation between demand and inertia does not hold.

[7] Same authors (see (P. M. Ashton et al., 2013)) previously used a fifth order polynomial. This has since been found to be unsuitable, as the fitting of the polynomial is too dependent on frequency effects well outside inertial time-scales, due to the curve having to be aligned with up to 20 s of data.

(Fan et al., 2013) proposes an inertia estimation method known as “finite difference method” which is based on PMU measurements, the classical generation model and the swing equation. It assumes that the PMU is located at an equivalent generator terminal (an area). Finite difference approximations of time derivatives of measured active power and estimated rotor angles are used. White noise affects derivatives computation by finite differences and needs to be filtered.

(Wilson et al., 2019) presents an online disturbance-based method for the measurement of effective inertia based on on the assumption that the power system can be considered as multiple centers of inertia, coupled through the network. The effective inertia of each area is identified by measuring the variation of the power flow through the area boundary and the area’s frequency. The method requires an area of the transmission system to be bounded by PMU measurements, such that the total net power flow into the area can be measured. Similarly, PMU measurements are also used to create an equivalent frequency to represent the area. Instead of using ROCOF, the effective inertia is calculated by integrating the power flow through the area boundary:

$$H_{Aeff} = \frac{\Delta p}{2 \cdot \frac{df}{dt}} = \frac{\int_{t0}^{t} \Delta p \cdot dt}{2 \cdot \int_{t0}^{t} df} = \frac{\int_{t0}^{t} \Delta p \cdot dt}{2 \cdot \Delta f} \tag{41}$$

Since estimation is time-varying, it must be post-processed by considering the linearity of the inertia function, time history, and precedence of lower inertia value estimates. A quality indicator is used to apply the method for smaller disturbances. Finally, a linear-relationship between areal effective inertia, demand and estimated total synchronous inertia is found. A similar approach is used by (GE, 2021).

(Federico Milano & Alvaro Ortega Manjavacas, 2020a) propose an inertia estimation based on the rate of change of power (ROCOP). The initial proposal computes the inertia by using the internal reactance of the generator, x_g, ROCOP and double-time derivatives of bus frequency, Δf_g, and ROCOP, $\dot{p}_g$, measured by a PMU:

$$H_g = \frac{-\dot{p}_g}{\frac{d^2}{dt^2}\left(\Delta f_g - \Omega_0 \cdot x_g \cdot \dot{p}_g\right)} \tag{42}$$

(Liu et al., 2021) extends the inertia estimation based on the rate of change of power (ROCOP), presented in (Federico Milano & Alvaro Ortega Manjavacas, 2020a) by providing two additional formulations that mitigate the numerical issues suffered by the initial proposal. The first formulation tackles the numerical issues by converting the initial algebraic estimation into first-order dynamic model, with variable, non-linear gain, depending on the double time-derivative of the rotational speed, and a time constant. This first-order model also acts as a filter. The second formulation includes the effect of the damping factor, by estimating it in parallel in a similar manner with a first-order dynamic model. Actually, the damping rather estimates the damping plus primary frequency regulation gain of synchronous generation or the primary frequency regulation gain in the case of non-synchronous generation using a VSM approach. The first formulation works fine for synchronous generation, whereas the second formulation works better for non-synchronous generation than the first formulation.

(Wall & Terzija, 2014) presents an algorithm to simultaneously estimate the time of disturbance[8] and the system inertia at that time. The estimation is based on the swing equations, neglecting the damping coefficient and approximating the mechanical power by the previously measured electrical power, and thus needs frequency and active power measurement of one single location. This is suitable for small systems but not necessarily for large systems. The selection of suitable locations is not addressed. The estimation of the inertia is based on four sliding data windows, two for frequency derivative and two for active power measurements. The time of disturbance can be extracted from the fact that measurements converge, which in turn is detected by analyzing the residuals between the last and the current estimations. Convergence issues due to damping can be mitigated by setting up an additional time-dependent band, where the estimate must fall. The algorithm depends on five user defined values (window length, residual threshold, etc.), which are system and event dependent. Noise and small window lengths (faster estimation) could also cause convergence problems. Increasing window length reduces the risk of false disturbance detection, but leads to overestimation of the time of disturbance and the inertia and increases computation effort. The residual threshold should be increased with increasing noise to ensure disturbance detection, but this increases the risk of false detection.

(Azizipanah-Abarghooee et al., 2019) proposes an online method to estimate the size of the active power unbalance and the system inertia simultaneously. The method is based on a modified swing equation of the COI, considering an estimation of the lost inertia. ROCOF of the COI frequency measurements after a disturbance are used to compute the inertial response, considering frequency dependency of loads, and the post-disturbance inertia. The size of the disturbance is interpolated from the inertial response over a time window of 1s to contemplate PMU measurement delays and measurement unreliability (e.g., frequency undershoot).

[8] The detection of time and size of the disturbance is critical for inertia estimation. (W. Wang et al., 2020) describes a method to detect the time of occurrence of a disturbance. The method filters frequency through a moving average window and it computes the frequency second derivative from the ROCOF, obtained both by applying fixed time windows to ROCOF and frequency measurements by PMUs. The time of occurrence is deduced from the minimum value of the second derivative. However, and although not mentioned, a threshold is needed to distinguish multiple consecutive disturbances. (Shams et al., 2019) presents a method to detect, locate and size a disturbance in the system. It does not require an inertia estimate. The method is fundamentally based on the distribution of the power disturbance among a set of generators, which depends on the relative synchronizing power coefficient, that in turn is related to the electrical distance. The method requires power measurement at a set of generators through PMUs and estimates the disturbance through the power disturbance distribution. The disturbance is detected by using a decision tree with respect to two indices making use of the power disturbance estimation. The location and size depend on one of the indices denominated normalized mismatch vector.

4.2.2.5 Modal analysis

According to 3.1.2, the inertia and the damping coefficient of the classical synchronous generator model are intrinsically related to the electromechanical oscillations quantified by the oscillation frequency and the damping. In case of multi-area systems, inter-area oscillations contain the inertia- and damping-related data. Typically, methods based on modal analysis tackle area-wide inertia estimation.

In (J. H. Chow et al., 2008) a parameter estimation method is developed, exploiting electromechanical oscillations. It assumes that the system can be separated into two areas with a transfer path between them and two PMUs installed at both ends. The method estimates first the reactance of the transfer path (by neglecting line resistance, being reasonable for transmission system), then the internal voltages and angles, and finally the system inertia by observing oscillation frequency. The values of the inertia for individual areas are obtained by observing relative speed variations.

(Guo et al., 2014) propose a methodology for online estimation of the parameters of a known dynamic power system model by employing the values of system modes, i.e., the modal frequencies and damping calculated from online WAMS measurements. It is assumed that the dynamic modes have been previously estimated. Modal sensitivity analysis is used to locate generators where parameter variations have most impact. The modal assurance criterion (MAC) pairs the observed oscillatory modes with those in the original model. A weighted least square estimation calculates the parameters by making use of the sensitivity matrix and, optionally, pseudo-measurements consisting of initial parameter value guesses. These guesses need to be accurate and some knowledge of the range of parameter variations is required.

(G. Chavan et al., 2017) describes a reduced-order, five-generator equivalent model of the Western Electricity Coordinating Council (WECC). The parameters of the model, i.e., equivalent inter-area line impedance, damping and inertia, and the generator reactance, are identified by extracting the slow oscillations using modal decomposition (e.g., prony analysis, etc.). Area equivalents are based on historical coherency; the pilot bus of each equivalent area need to be equipped with a PMU, all area generators need to be behind that bus, and pilot buses of different areas need to be connected. Whereas the impedance of the line and the reactance can be estimated by means of voltage and current measurements, damping and inertia are estimated from the slow oscillations by formulating a least square problem.

In (Cai et al., 2019), the extraction of the oscillation’s parameters (damping and frequency) is carried out by means of an adaptive local iterative filtering decomposition (ALIFD). Further, the method supposes oscillations between two areas, which in case of multi-area systems have been obtained by an appropriate network reduction including coherency.

(Yang et al., 2020) presents an area-based inertia estimation approach by using ambient data measured by PMUs. Inertia estimation is based on the modal information of inter-area oscillations. A two-generator equivalent of an interconnected power system is identified and constructed for a particular mode. Electrical power interchange is measured directly, whereas internal angles are deduced from the current injection phases. The modal information (eigenvalue and right eigenvector, extracted from the average frequency) is obtained by means of the recursive adaptive subspace identification and determines the total two-generator equivalent inertia. The inertia of each Individual area is obtained by knowing the definition of the equivalent inertia and the inertia-relationship, depending on the eigenvalue and right eigenvectors. Identification of equivalent two-generator systems might not always be feasible and could lead to significant errors.

(Wang, B. et al., 2020) describes an online inertia estimation algorithm that uses of ambient data to extract modal information on the electromechanical oscillations. From the autocorrelation power spectral density, showing two peaks under white noise excitation, it can be inferred, that oscillations are contained in ambient response. The modal information is extracted from ambient data obtained through PMU measurements by means of stochastic subspace identification (SSI). PMU measurements are angle (internal angle) and electrical power of each generator. Simulations and experiments for a single-generator to infinite bus system show the applicability of the method.

(Panda et al., 2020) describes an online method to estimate element and area inertia using a known or detected disturbance. VSMs can be contemplated. The method uses PMU frequency measurements, and modal information is extracted by means of a method called estimation of signal parameters via rotational invariance techniques (ESPRIT), requiring a predefined model order (number of modes). An equivalent mode of detected modes is derived by computing the *qth* coefficients of the discrete Fourier transform of a given window. Since the sum of the modes of the frequency provides the frequency signal, the sum of the *qth* coefficients of the Fourier transform of each mode gives the *qth* coefficient of the Fourier transform of the frequency signal. Inertia is then computed based on the swing equation and by using the damping and frequency deduced from this *qth* coefficient, the measured active power variations, and the computed (not measured) ROCOF. Window length, selection of *q*, and model order are critical. Selection of *q* seems to be oscillation frequency related, but no guidelines are given. Initial measurement samples are discarded to avoid phase jumps in the measurements of PMUs.

(Yang et al., 2021) presents a disturbance-based estimation of area effective inertia by extracting inter-area modal information from PMU measurements. The estimation assumes the existence of coherent areas that can be represented each by the swing equation. Speed deviations and electric power deviations of each area should be measured, where speed deviations are approximated by the weighted-average area frequency and the electric power by the sum of the power in the tie lines. Dynamic mode decomposition (DMD) is used to extract from two snapshots of matrices of measurements the eigenvalues and DMD modes (eigenvector). The swing equation can then be re-written in terms of the DMD modes of the speed and electric power deviations and, thanks to their complex-valued nature, the inertia and damping can be computed. Appropriate modes need to be extracted from the measurements.

4.2.2.6 Artificial neural networks

Since the inertia estimation as any parameter identification problem can quickly become very complex due to limited measurements, simplifications of the underlying model and phenomenon, etc., artificial neural networks (ANN) have been proposed for this purpose. ANN need to be previously trained.

(A. Schmitt & B. Lee, 2017) describes the use of an ANN to estimate system, area and bus inertia under normal operation conditions. The ANN's input consists of modal information of the oscillations inherent in frequency measurements at buses. Empirical mode decomposition applied to the frequency measurements of a time window of 2 seconds provides modal frequency and damping. The ANN has been trained by simulating hundreds of different cases where system fluctuations have been caused by random load variations and by extracting the first four modes. Whereas area and system inertia could be predicted relatively well, bus inertia prediction is far less accurate since relation between modal information and individual bus inertias is less clear.

In (Hartono et al., 2019), the ANN is trained and tested with the frequency responses of a system that have been simulated with several inertia values and subject to various disturbance magnitudes. The extension of the simulation campaign and the details of the underlying model are unknown.

In (E. S. N. R. Paidi et al., 2020), a wide range of scenarios of wind generation penetration and load cases have been contemplated to train an ANN. For each scenario and case, a system equivalent inertia has been derived from the inertia parameters of SGs and the other components in the system that contribute to the inertia. A Pearson correlation analysis has shown that the total active power generation from all synchronous generators, total active power produced by all non-synchronous generators, and total dynamic induction motor power, measured by PMUs through WAMS, are the most suitable input variables for the ANN. PMU measurements have been simulated in DigSILENT and RTDS.

4.2.2.7 Stochastic estimation

The amount of available system inertia can be represented as a result of several stochastic processes. Furthermore, measurements and estimations are always subject to uncertainties.

(X. Cao et al., 2016) presents a switching Markov Gaussian model (SMGM) to estimate system inertia online during normal operation conditions by using the steady-state frequency as input. The complex stochastic interdependency of frequency and inertia suggests the use of Gaussian mixture models. Parameters of the Gaussians are determined according to the expectation maximization, and the number of mixtures according to the minimum Bayesian information criterion. Temporal dependence is encoded as mixed-order Markov chains. The "skip k transition autoregression" technique determines which prior states are regressive with the current state. Slice sampling is used to draw samples from the mixture distribution. SGMG is trained using historical data. A fourth-order SMGM seems outperform a mixture model only. A periodic online re-calibration is needed to limit the accumulated inertia estimation, which uses dispatch information therefor. Further, the method is dependent on a set of parameter and choices (number of mixtures, conditional distribution covariance matrix, sampling selection approach, etc.). It is not valid during disturbances.

(N. Petra et al., 2017) proposes a Bayesian disturbance-based approach to estimate the inertia with uncertainty. The solution of the Bayesian inverse problem quantifies through computing the statistics of the pdfs how much information from the measurement data can be used to identify the inertia. A local Gaussian approximation of the posterior around the maximum a posteriori (MAP) point of the inertia and its variance is used therefor. Two methods are proposed to compute the MAP and parameter uncertainty: (i) adjoint-based method and (ii) stochastic spectral method. The approach has been applied to a 9-bus system. Bus voltage is measured and an estimation window of 1 s seems to be sufficient. Larger perturbation reduce variance. Stochastic spectral method seems to be less demanding in terms of computation effort. Fewer measurements points (less observations) have low impact. Larger system requires further work.

(Allella et al., 2020) proposes a method which uses a stochastic process to estimate the system inertia. It is assumed that non-synchronous generation does not provide inertia. The inertia is modeled as the sum of periodic components and a weakly stationary stochastic process distributed according to a logistic distribution. The model is trained by inertia measurements obtained according to the breaker status (SCADA) and the knowledge of individual inertia constants. The measured inertia shows periodic components of 24, 12, 6 and 4 hours obtained through Goertzel's method. The measurements, corrected by subtracting the periodic components, are then used to identify the stationary process by means of a first-order auto-regressive model.

4.2.2.8 Kalman filters

Kalman filters (KF) have been widely applied for dynamic state estimation and parameter estimation. EKF enhance KF by considering nonlinear models that are linearized. A central and vital operation performed in the KF is the propagation of a random variable through the system dynamics. In the EKF, the state distribution is approximated by a random variable, which is then propagated analytically through the first-order linearization of the nonlinear system and which could introduce errors in the true posterior mean and variance of the transformed random variable. (Vieyra et al., 2020) uses the UKF to estimate the dynamic states of an islanded microgrid, described by a set of algebraic differential equations (DAEs). The UKF calculates the statistics of random variables that undergo a non-linear transformation since it is easier to approximate a distribution function than to approximate the nonlinear transformation. To incorporate parameter estimation within the KF, the model needs to be augmented (e.g., (Z. Huang et al., 2013) and (Fan, Lingling & Wehbe, 2013).

(Ariff et al., 2015) proposes an approach to estimate dynamic model parameters by processing PMU measurements through an UKF. A classical generator model has been used a priori with constant mechanical power, augmenting the state vector by its parameters and process noises of active power and voltage measurements. Covariance matrixes of process and measurements noise are assumed to be constant and known. PMU measurements at every generator terminal are assumed to be known, too. Parameter and state variables are estimated within 1 s. The results have been compared with EKF ((Z. Huang et al., 2013) and (Fan, Lingling & Wehbe, 2013)), leading to faster and more robust estimations.

(Zhao et al., 2019) proposes a method to estimate rotor angle, speeds and inertia in an online manner to finally estimate the frequency of the COI. The generator active power and rotor speeds need to be measured by or estimated through PMUs measurements. The method is based on a discretized version of the generators' swing equation and makes use a modified Kalman filter approach (to account for measurement losses and outliers (J. Zhao et al., 2017)) for the joint estimation of generator rotor speed, angle and inertia constant. The joint estimation of the inertia augments the state variables by the inertia (see (Ariff et al., 2015)). Estimating the inertia simultaneously improves estimation of COI frequency. In (Wang, X. et al., 2020), a similar approach to (Zhao et al., 2019) is used to estimate online the rotor angle and speed.

4.2.2.9 Disturbance injection

Whereas previous methods make use of event-based disturbances or ambient data, other methods actively perturb the power system. This has the advantage of knowing the disturbance precisely, whereas the active injection of a disturbance might pose a problem at the same time. Typically, these approaches make use of methods similar to those in sections 4.2.2.3 and 4.2.2.4.

(J. Zhang & H. Xu, 2017) proposes a real-time online equivalent inertia constant identification method. A closed-loop microperturbation method (MPM) is proposed. The closed-loop MPM uses PMU measurements to estimate the system inertia constant from the bus at which the system is connected to. The MPM injects a multisine probing signal with sufficient energy with respect to possible noise by means of a power electronic device (inverter, AVR, etc.). Inertia is then estimated by identifying two transfer functions by means of the orthogonal decomposition-based subspace method and then dividing them: (i) between the frequency and the signal, and (ii) between active power and the signal. Frequency response fitting is finally used to reduce the measured transfer function to the equivalent transfer function and to extract the inertia. Unlike indicated, the method seems to estimate the inertia of elements and not the system as a whole.

(Best et al., 2021) estimates the system inertia by making use of known perturbations, caused by the flow changes on a HVDC interconnector. The method makes use of the kinetic energy rather than the inertia. It measures energy variation due to the perturbation and frequency between two instants. The paper suggest that the measurement should not be taken to early since initial transients affect computation and frequency measurement. Energy variation is computed by integrating perturbation power corrected by an estimate of the system response, modelled as a time delay with linear response (see (I. Egido et al., 2009)). Frequency is measured over 500 ms moving average. The paper also quantifies the inertia of auxiliary power station loads (around 10% of generator inertia) and of the demand (see (Bian et al., 2018)).

(S. Shah & V. Gevorgian, 2019) proposes a system inertia estimation making use of a frequency response function between a known active power injection and the measured frequency at the point of injection. The frequency response function is obtained by injecting sinusoidal power perturbation with a given frequency by for instance a battery storage system and measuring the corresponding system frequency. For each perturbation frequency, the corresponding Fourier coefficient of the power and the system frequency are used to compute the response function. A resonant dip in the frequency response function is related to the inertia. How the inertia is extracted from the peak is not fully clear. It is also shown that the system frequency response is related to the dq-domain impedance of the network.

A commercial product on inertia estimation also actively injects an active power disturbance and measures frequency deviations at different parts of the network (Berry, 2019). Inertia estimation is based on the swing equation.

4.2.3 Inertia distribution

Most of the reviewed approaches focus on inertia estimation, i.e., the amount of inertia available, but do not directly consider inertia distribution. A first step in this direction is given by splitting the system into predefined areas, providing a rough estimation of the inertia distribution. The use of modal analysis inherently considers the distribution of inertia since oscillation frequency of modes not only depends on the inertia but also the electrical distance, i.e., the grid (see sections 3.1.2 and 3.2). (Pagnier & Jacquod, 2019) has shown that the slowest network mode, called Fiedler mode, has a large impact, and adding inertial response in Fiedler areas (areas participating in the Fiedler mode) is beneficial.

4.2.3.1 Indices

Inertia distribution can be determined by means of indices. (Wang, Y. et al., 2017) describes two indices to calculate the distribution of inertia. For a perturbation at each bus, the first index uses the difference of synchronous machine speeds, whereas the second index uses the difference of the bus frequency and the frequency of the COI. These indices help determining the closest (minimum index) and furthest (maximum index) location from COI, and regions with similar indexes. Measurements of all machine speeds and bus frequencies are needed. In fact, the difference of the bus frequency with respect to the COI frequency is measured rather than the actual inertia distribution. However, a frequency close to the one of the COI indicates that the corresponding bus is close to the COI.

(Pulgar-Painemal et al., 2018) studies the location of non-synchronous elements that are enabled with either damping controllers or inertia emulation controllers. The paper analytically derives an expression for a simple two-generator system that relates the COI with an electrical location. The relative distance of the COI is inversely proportional to the relation of the inertias of the two generators. The eigenvalue sensitivity, expressed in terms of the residue and the controller transfer function when written in explicit hybrid form, shows that the residue is larger (i.e., the sensitivity) for larger relative distances. For larger system, the inertia distribution index is introduced, using the difference between the bus frequency and the COI frequency (see (Wang et al., 2017)). The index allows defining inertia regions according to the similarity of the index (called layer, requiring expert knowledge). Bus and generator frequencies are needed. Further, the index and the residue seem to be correlated.

(Xiao et al., 2019) assesses the spatial and temporal distribution of system inertia. Together with the results of a unit commitment (UC) and the PMUs measurements, two indexes are computed: (i) the rate of change of inertia with respect to the non-synchronous generation penetration, and (ii) the inertia distribution index (as in (Wang et al., 2017)), which takes into account the sampling period of the PMUs.

(Brahma & Senroy, 2021) defines two indices to quantify the dynamic grid flexibility of a power system. Dynamic grid flexibility merges operational flexibility and small signal stability. The two indices are: inertial index and dynamic flexibility index. The former is defined as the sensitivity of the critical electromechanical eigenvalue to active power injection, whereas the latter is computed by multiplying the row-wise sum of the inertial sensitivity matrix (partial derivatives of the bus angles to the generator angle and generator speed) and the right eigenvector of the critical eigenvalue. The angle information of the inertial index of all buses can be used to categorize all the buses into coherent bus groups. A large inertial index indicates that bus angles strongly vary with generator angles and speeds. This looks similar to the index in (Wang et al., 2017).

4.2.3.2 Bus distribution

(You et al., 2018) presents a non-invasive approach to measure system inertia distribution by using frequency measurements from PMUs. It makes use of the non-uniformity of the electromechanical wave propagation speed during active power imbalances. The continuum model was used to analyze wave propagation, that describes an inverse relationship between the inertia (of per unit length of the continuum model) and the propagation speed, evaluated through the time of arrival at different PMUs. Since PMU coverage is incomplete, measurement interpolations are used. Data quality and timing issues make necessary to check the measured time of arrival by applying a linear regression between the measurement point and the estimated location of the disturbance (smallest time of arrival calculated).

(Zeng et al., 2020) estimates bus inertia from ambient data. By making use of the frequency divider (Federico Milano & Alvaro Ortega Manjavacas, 2020a) and the swing equation, the bus inertia depends on the generator's inertia values and on the electrical distance of the bus to each one of the generators. First, the generator transfer functions, relating generator active power and a bus frequency deviation, are identified through a subspace identification method and by measuring electrical power at each generator and the frequency at the bus of interest *j*. Virtual inertia could be considered. Instead of reducing the transfer function to the one of the swing equation, the identified transfer functions are simultaneously excited with a unit step input and the bus inertia can be computed from the derivative of the rotor speed variations together with the electrical distance m_{gj},:

$$h_j = \frac{1}{\sum_g \frac{m_{gj}}{H_g}} \tag{43}$$

where

$$\begin{aligned} \sum_g \frac{m_{gj}}{H_g} &= \sum_g -m_{gj} \frac{d\Delta\omega_g}{dt} \\ &= -\sum_g L^{-1}\left\{ s \cdot G_{gj}(s) \cdot \frac{1}{s} \right\}\Bigg|_{t=0} \end{aligned} \tag{44}$$

and

$$G_{gj}(s) = \frac{m_{gj}}{2H_g s + D_g} \tag{45}$$

The approach computes the inertia distribution since bus inertia values are not independent; it looks like an inertia divider.

5 Discussion

This section discusses the needs and assumptions behind inertia estimation methods. Since inertia estimation is a parameter-identification problem, the suitability of the underlying model, the exciting trigger signal and measurements used are key issues to be considered. Discussion turns thus around:

- Measurements
- Trigger signal
- Models
- Methods
- Scope and distribution

The applicability of inertia estimation methods to distribution system is finally discussed.

5.1 Measurements

Most of the inertia estimation methods are based on PMU measurements. These measurements when within a WAMS are synchronized, time-stamped measurements. For both online and offline estimation methods, the availability of synchronized, time-stamped measurements is of paramount importance since time shifts induce estimation errors. Measurements should have sufficient resolution and accuracy. The fundamental frequency sampling rate of PMUs seems to be sufficient (sampling frequency should be at least 8 Hz (Tavakoli et al., 2012)). In Ireland, fast frequency response (FFR) recorders are required to have a time resolution of 20 ms and a time synchronization accuracy of 2 ms.

Since measurements suffer from noise, measurements are filtered. Moving average filters, sliding window filters, median filters, Butterworth filters, etc., have been proposed. The computation of ROCOF from the frequency could further accentuate noise and oscillations. Commonly, Butterworth filters have a 0.5 Hz cut-off frequency, which filters out some of the electromechanical oscillations present in the measured signal. The impact of the window length has been analyzed in addition to the impact of noise level. Increasing the window length leads to overestimation of the inertia and increases computation effort (Wall & Terzija, 2014). The comparison of two estimation methods has shown that shorter window length is beneficial for disturbance-based estimations (Kontis et al., 2021). It seems that ARMAX models work better under moderate noise levels, whereas it might fail to provide inertia estimations under high noise levels. For moderate noise levels, window lengths seem to be bounded. Whereas both methods work well under different disturbance magnitudes, the sliding-window-based approach seems to be more robust against varying disturbance locations and its window length are hardly influenced by the locations. (Lugnani et al., 2020) suggest determining the post-disturbance window length to minimize the estimation variance. Further data treatment might be needed to tackle PMU measurement delays and measurement unreliability such as the measurement-induced frequency undershoot.

Whereas the deployment of PMUs throughout the transmission grids is increasing, their use in distribution grids is far less common. Many approaches initially used a single frequency and/or disturbance power measurement to estimate inertia. A single-node frequency measurement is however usually not sufficient unless measured very close to the COI. The COI is however time and spatial varying according to the unit commitment of generating units. COI frequency can be approximated by weighting frequency measurements taken at well chosen locations (KUIVANIEMI M. et al., 2015). In this regard, PMUs can help providing synchronized frequency measurements at several locations to be processed. Some methods require however a very dense PMU measurement grid, even at every terminal (e.g., (Ariff et al., 2015), (Zhao et al., 2019), (Sun et al., 2019))

The estimation of system inertia from estimated area inertia is a particular application, where the time and spatial variation translates into the determination of the area and its boundary. The location of PMUs is thus of particular concern. Experience or coherency-based solutions have been used. PMUs should not be collated too close to the disturbance since it might corrupt measurements, worsening the results of approaches based on the assumption of small differences between speed and generator terminal frequency. (Lara-Jimenez et al., 2017) presents a method to determine suitable PMU measurement locations for inertia response estimation. Generator groups that form aggregated sources of inertial response are identified, as well as their inertial centers, where PMUs should be placed. These groups are obtained by applying a graph theory-based spectral clustering algorithm. Dynamic graph edge weights are defined, depending on the inertia, the electrical distance, and the angle difference. Eigenvectors (spectrum) of the graph's Laplacian and the eigengap are used to obtain the number of clusters. The inertia center of each group can be computed in terms of the electrical distance among the non-generator buses within the group or in terms of an inertia-weighted electrical distance among generator and non-generator buses. The inertia-weighted approaches provide better results. Similarly to coherency-based solutions, the method requires the knowledge of the inertia of the generators connected, where their commitment status can vary significantly.

5.2 Trigger

Inertia estimation has been divided into event-based estimation and continuous estimation. Estimation algorithms can run online or offline, where offline algorithms are mostly event-based. The trigger of the estimation can be (i) a ringdown signal (large disturbances), (ii) ambient signal (continuous small disturbances), (iii) and probing (injection) signal. Methods requiring a significant event (large disturbance) suffer from the inherent drawback that such disturbances luckily do not occur often.

Many inertia estimation approaches are based on a ringdown signal, i.e., they require the presence, detection and identification of a sufficiently large disturbance. Initially, most approaches assumed known disturbances, which was a suitable assumption for offline inertia estimation (e.g., after a large incident). The significance of the disturbance has been assessed through the ROCOF, by comparing the measured value with a threshold. Suitability of an event can also be determined by a detrended fluctuation analysis (DFA), comparing fluctuations with a threshold. In (Ashton et al., 2015), a suitable event is chosen when the fluctuation decreases below the threshold within 1 s.

Nonetheless, for online estimation methods, the size and instant of the disturbance is not usually known. Sometimes, the disturbance can be measured. For instance, for well defined areas (in its limit case, a grid connected to another one through a single line), the boundary power flows in addition to the frequency and voltage could be measured, providing an estimation of the area unbalance. If areas cannot be previously defined or not sufficient measurement points are available, inertia and disturbance (size and instant) can be estimated simultaneously. (Wall & Terzija, 2014) presents an algorithm to simultaneously estimate the instant of disturbance and the system inertia at that time. (W. Wang et al., 2020) describes a method to estimate the time of occurrence of a disturbance, whereas (Shams et al., 2019) presents a method to detect, locate and size a disturbance in the system. It does not require an inertia estimate. (Azizipanah-Abarghooee et al., 2019) proposes an online method to estimate the size of the active power unbalance and the system inertia simultaneously. The size of the disturbance is interpolated from the inertial response over a time window of 1s to contemplate PMU measurement delays and measurement unreliability.

5.3 Models

In most references, the underlying model is given by the swing equation, representing either the system, an area, or an element. The damping term is mostly neglected. A sufficiently accurate estimation of the disturbance and of the ROCOF would allow estimating the inertia. Indeed, this approach could be appropriate for a synchronous machine and/or loads. With respect to loads, (Best et al., 2021) quantifies the inertia of auxiliary power station loads around 10% of generator inertia) and of the demand.

However, the swing equation as such neglects other responses within the system such as those of loads to a disturbance. (Zografos et al., 2018) considers both frequency and voltage dynamics of the system, and in particular voltage and frequency dependence of the load. (Phurailatpam et al., 2020) uses a curve-fitting approach to consider load variation. Other modifications contemplate the estimation of an equivalent droop through solving a linear set of equations with augmented measurements (Zografos et al., 2018) or the direct modeling of primary frequency control (e.g., (Schiffer et al., 2019) or (Best et al., 2021)). Finally, (Tuttelberg et al., 2018) coins the term *effective inertia* to include virtual or emulated inertia and voltage and frequency dependency of loads. The effective inertia actually relates active power variations with ROCOF. However, notice that voltage and frequency dependence of loads *per se* do not contribute to inertia itself but to the reduction of the size of the disturbance (e.g., frequency-dependent loads do not oppose to power variations but reduce power consumption if frequency drops).

Some works include high-order models, mainly of synchronous generators, adding excitation dynamics to the individual swing equations. Especially for approaches based on Kalman filters. Individual swing equations coupled through grid equations, mostly lossless, can be found in approaches making use of modal analysis. Regardless the detail of the individual or (system/area) equivalent synchronous generator, penetration of non-synchronous devices that could provide inertia has seldom be contemplated directly. (Phurailatpam et al., 2020) highlights that its approach loses accuracy since inertia emulation is not instantaneous and thus different to inertial response of synchronous generation. (Zeng et al., 2020) states that virtual inertia could be considered but does not provide further insight. Finally, (Fernández-Guillamón et al., 2019) compares different system inertia methods and their applicability when non-synchronous generation provides virtual inertia (inertia emulation). In particular, the impact of emulating inertia by means of temporary overproduction (TOP) of wind power plants is studied. The results show that the methods considered provide reasonable estimates when the non-synchronous generation does not provide virtual inertia. However, only the method reported in (Wall & Terzija, 2014) provides an appropriate estimation of the system inertia. One possible reason is that TOP hardly influences the initial ROCOF but rather subsequent instants. Considering sliding windows as in (Wall & Terzija, 2014) around the estimated instant of the disturbance seems to be beneficial. For estimation methods relying on a model, it seems important that such models capture the dynamics, i.e., TOP. This will be especially true for Kalman filter based methods.

5.4 Methods

Static and dynamic inertia estimation methods have been reported. Static estimation makes use of static information, i.e., the monitor breaker status of generation units and combine the breaker status data with the corresponding inertia value, extracted from a data base. The drawback lies in the need for accurate and updated data base and in the difficulty the breaker status of all generation units.

In turn, dynamic estimation uses recorded responses of the system. Most dynamic inertia estimation methods can be grouped according to the underlying phenomenon: electromechanical oscillations or speed acceleration. Inertia estimation can also be understood as a part of equivalent dynamic network modeling, providing however only a single inertia value. Independent of the scope, different methods based on the swing equation have been proposed. The swing equation has been reformulated such that energy and frequency measurements can be used for its evaluation ((Tavakoli et al., 2012), (Wilson et al., 2019)). (Federico Milano & Alvaro Ortega Manjavacas, 2020a) propose an inertia estimation using the rate of change of power (ROCOP), based on a further time derivative of the swing equation. Polynomial approximation of different orders for frequency and powers have been proposed, which are then used within the swing-equation model. The proposed polynomial fitting requires longer measurement horizons and depend on other effects outside inertial time scales. Instead of using a polynomial fit of the frequency, ROCOF can be computed through finite differences (Fan et al., 2013) or even by building a discretized linear (frequency) model (Sun et al., 2019), solved by the least square method. Transfer functions have been directly identified online by implementing ARMAX models, requiring non-linear optimization such as gradient-based method to solve for the parameters to be estimated. Non-linearities such as limits, dead bands, etc. can however affect the estimation under large disturbances, Hammerstein-Wiener models have been proposed to capture the input and output non-linearity of the previously identified linear models (Phurailatpam et al., 2021).

Approaches based on modal analysis inherently require some more detailed modeling. Typically, system models are reduced to known, previously defined multi-area models or equivalent two-generator models are within the estimation process. Model reduction has been based on coherency or the identification of transfer paths as in (J. H. Chow et al., 2008). The identification of equivalent two-generator systems might not always be feasible and could lead to significant errors. (Guo et al., 2014) assumes that modes have been previously identified and computes parameters with a least square method and by using a modal sensitivity matrix. The modal assurance criterion pairs the observed oscillatory modes with those in the original model. Several references focus on the identification of the modes and propose different methods therefor: adaptive local iterative filtering decomposition (ALIFD), subspace identification, estimation of signal parameters via rotational invariance techniques (ESPRIT), dynamic or empirical mode decomposition, etc.

Kalman filters (KF) have been widely applied for dynamic state estimation and parameter estimation. EKF and UKF extend the traditional KF to include non-linearities and to avoid errors due to the approximation of the nonlinearities affecting the propagation of the random variable, respectively. KF requires covariance matrixes of process and measurements noise, which are assumed to be constant and known in many cases (e.g., (Ariff et al., 2015)). Typically, KF-based approaches use classical generator models or reduced-order models to estimate, among others, inertia.

Apart from model-based approaches, inertia estimation methods making use of ANN or exploiting stochastic processes have been proposed. ANN have been trained by using modal information or system responses in terms of frequency as input variables, aligned with the classification of the underlying phenomenon. Whereas area and system inertia could be predicted relatively well in (A. Schmitt & B. Lee, 2017), bus inertia prediction is far less accurate since relation between modal information and individual bus inertias is less clear. In (E. S. N. R. Paidi et al., 2020), a correlation analysis has shown that measurements of total active power generation from all synchronous generators, total active power produced by all non-synchronous generators, and total dynamic induction motor power are the most suitable input variables for an ANN estimating a system inertia. However, the measurement of the total induction motor power or even of all generators is not necessarily available. Changing and non-contemplated scenarios affect accuracy of ANN in general.

Training is also needed for the methods exploiting stochastic processes. (X. Cao et al., 2016) suggests using a Switching Markov Gaussian model (SMGM) to consider the complex stochastic interdependency of frequency and inertia, represented by Gaussian mixture models, and the temporal dependency, addressed through Markov chains. SGMG is trained using historical data, but a periodic online re-calibration based on dispatch information is needed to limit the accumulated inertia estimation. Dispatch information, i.e., breaker status and corresponding inertia constant, is also needed to train the inertia model proposed in (Allella et al., 2020), where inertia dynamics are the sum of periodic components and a weakly stationary stochastic process.

As mentioned in section 5.2, some methods actively inject a probing signal, disturbing the system. Existing devices such as HVDC converters or AVR of generators can be used, but also new devices such as battery energy storage systems or ultracapacitors have been suggested for this purpose (Berry, 2019). Sine or multisine probing signals are used. (J. Zhang & H. Xu, 2017) identifies from the response to the probing signal transfer functions and applies frequency response fitting to finally extract the inertia. A frequency response function obtained by computing the Fourier coefficient of the power and the system frequency for each perturbation frequency is used in (S. Shah & V. Gevorgian, 2019). How the inertia is extracted from the peak is not fully clear since it requires the quantification of the equivalent inductance of the external grid for which inertia is estimated.

5.5 Scope and distribution of inertia

Inertia estimation methods have been classified into system-wide, area-wide and element-wise estimation methods. The estimation of the system-wide inertia provides valuable input with respect to its robustness in terms of frequency variations to active power unbalance. A single, system-wide is however not able to provide more insight into the distribution of the inertia within the system. A first step in this direction is given by splitting the system into predefined areas, providing a rough estimation of the inertia distribution. The use of modal analysis inherently considers the distribution of inertia since oscillation frequency of modes not only depends on the inertia but also the electrical distance, i.e., the grid.

The distribution of the inertia within the system has only recently attracted some attention. Most of the reviewed works determine a distribution indexes. Some indices measure generator speed differences or the differences of certain bus frequencies with respect to the frequency of the COI. The rate of change of inertia with respect to non-synchronous generation penetration has also been proposed as an index. An inertial index, assessing the sensitivity of the critical electromechanical model to active power injection, has been defined in (Brahma & Senroy, 2021). The angle information of the inertial index of all the buses can be used to categorize all the buses into coherent bus groups. A large inertial index indicates that bus angles strongly vary with generator angles and speeds. These indices have in common that they show the relative distribution but not the absolute one. The application of these relative distribution indices to an estimated amount of inertia (e.g., system inertia) to derive the absolute distribution has not been shown so far.

Two papers tackle the estimation and measurement of inertia distribution. One makes use of the non-uniformity of the electromechanical wave propagation speed during active power imbalances. The time of arrival at different PMUs approximates the propagation speed, being inversely proportional to the inertia. The second approach makes use of the frequency divider formula and estimates bus inertia from ambient data. Actually, individual generator transfer functions between the frequency of a given bus and the generators active power are identified by a subspace identification method and their joint excitation with a unitary step response allows estimating a given bus inertia. Care should be taken since bus inertias are not independent from each other, so neither this approach provides an absolute inertia distribution.

5.6 Applicability to distribution systems

Inertia estimation methods mainly focus on the bulk power system. It is however true that these methods have different scopes (system-wide, area-wide or element-wise) and that these methods could be potentially applied to the estimation of the inertia within a distribution system. Indeed, a distribution system could be, at least conceptually, considered as an area, for which inertia estimation methods have been developed.

An important question is whether a single value of the inertia of the distribution system is sought or whether a deeper insight is needed, highlighting the distribution of the inertia within the distribution system. Equivalent dynamic models of active distribution networks (ADN) have been widely developed and discussed. However, such models only provide an equivalent inertia or equivalent inertia values disaggregated according to generation and demand, and their technology (e.g., an induction machine in parallel with a composite load and a converter-connected generator. (J. V. Milanović & S. Mat Zali, 2013)). The same comment applies to those methods that make use of frequency and area-boundary power measurements to determine inertia (e.g., (Wilson et al., 2019) or (Tuttelberg et al., 2018)).

The application of inertia distribution methods to distribution systems could provide further insights. However, these methods provide relative distribution indexes or bus inertias, which are not independent from each other. In addition, PMU measurements at different locations would be needed. The deployment of PMU in distribution systems clearly lags the one in bulk power systems. A PMU at the point of common coupling of the distribution grid, measuring voltages and frequencies and active and reactive power flow could only determine the equivalent inertia of the distribution grid. A more detailed picture could be obtained by deploying further PMUs for instance nodes where the grid branches. Figure 4 illustrates this idea for a very simple case. The up-stream PMU could determine the equivalent inertia of the distribution grid, whereas the down-stream PMU determines the down-stream inertia. The inertia of the other branch without PMU could then be obtained by simple subtraction. Without being exhaustive, inertia estimation methods such as the ones proposed in (Tuttelberg et al., 2018), (Fan et al., 2013), (Wilson et al., 2019), (Federico Milano & Alvaro Ortega Manjavacas, 2020a), etc. could be used to evaluate the inertia down-stream of a PMU. These methods estimate the equivalent inertia since they are based on the swing equation. Ideas of (Zografos et al., 2018) on including load-response, etc. could be also accounted for. Kalman filter as in (Ariff et al., 2015) or (Zhao et al., 2019) could also be used, but the underlying model will be, at most, an equivalent representation since exact number, type and connection status of downstream generation units are usually not known by DSO.

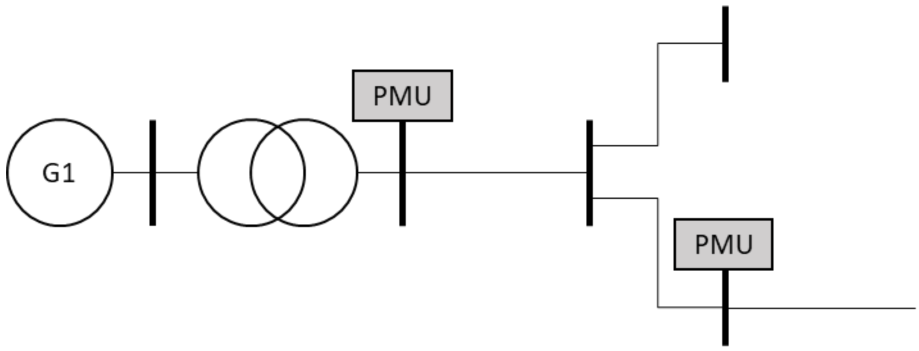

Figure 4: Illustration of the location of PMUs at grid branching nodes.

Approaches making use of modal analysis can provide additional insights into the distribution of the inertia. Indeed, the oscillation frequency of the modes depends on the inertia and its electrical distribution. Modal analysis requires the detection and identification of the modes. In case of distribution systems, there exist local modes as well as inter-area modes. One of the inter-area modes corresponds to the oscillations of the distribution system against the remaining system. Oscillation frequencies of local and inter-area modes are typically different. The inter-area mode of the distribution system against the remaining one could allow estimating the inertia of the distribution system (as well as the one of the system) using, for example, the method of (J. H. Chow et al., 2008). Approaches reported in (Guo et al., 2014) or (Panda et al., 2020) could also be used as candidates. Note that if the *n-1* independent electromechanical modes of a *n*-machine power system were measurable, only *n-1* inertias could be estimated.

Generation technology in distribution systems include both synchronous and non-synchronous generation, where the latter is increasing continuously. Since inertia estimation is a model identification problem, all methods suppose an underlying model, ranging from a single swing equation based model to reduced-order multi-synchronous generator models. The performance of the methods and particularly of methods based on modal analysis and Kalman filtering depend on the appropriateness of the model. Indeed, the response of non-synchronous generation is very different to the response of synchronous generation. However, control approaches of non-synchronous, grid-forming generation making use of virtual synchronous machine implementations, droop controls, etc. emulate a behavior of synchronous machines. Apart from modeling assumption, knowledge of connection status and measurements are needed, the more the better as in the case of proposed Kalman filtering methods.

Although stochastic estimation or methods based on ANN do not necessarily require very accurate dynamic models, they need on extensive training by using historical data or off-line simulations (A. Schmitt & B. Lee, 2017), (E. S. N. R. Paidi et al., 2020), (X. Cao et al., 2016). These methods or rather their data bases need to be periodically updated to catch operation conditions and structural changes not considered initially. Periodic online re-calibration could be needed to limit the accumulated inertia estimation.

Given the limited amount of PMU measurements available in distribution systems and the complexity of certain approaches (e.g., modal-analysis-based or KF-based estimations), one could recommend inertia estimation methods based on the swing equation or approaches used to identify equivalent dynamic models of ADN to start with the implementation of inertia estimation methods in distribution systems. These approaches are relatively simple to implement and with certain degrees of maturity. The drawback is that with a single measurement location, only total inertia of the distribution system can be estimated. A more detailed picture could be obtained by deploying further PMUs for instance nodes where the grid branches (see Figure 4).

6 References

[1] Mehigan, L., Dlzar Al Kez, Seán Collins, Aoife Foley, Brian Ó'Gallachóir, and Paul Deane. 2020. "Renewables in the European Power System and the Impact on System Rotational Inertia." *Energy* 203: 117776. doi:https://doi.org/10.1016/j.energy.2020.117776. https://www.sciencedirect.com/science/article/pii/S0360544220308835.

[2] Nikolic, Dusan and Michael Negnevitsky. 2019. "Adding Inertia to Isolated Power Systems for 100% Renewable Operation." *Energy Procedia; Renewable Energy Integration with Mini/Microgrid* 159: 460-465. doi:https://doi.org/10.1016/j.egypro.2018.12.040. https://www.sciencedirect.com/science/article/pii/S1876610218313353.

[3] Osbouei, B. A., G. A. Taylor, O. Bronckart, J. Maricq, and M. Bradley. 2019. "Impact of Inertia Distribution on Power System Stability and Operation.". doi:10.1109/PTC.2019.8810689.

[4] Kryonidis, Georgios C., Eleftherios O. Kontis, Theofilos A. Papadopoulos, Kalliopi D. Pippi, Angelos I. Nousdilis, Georgios Barzegkar-Ntovom, Alexandros D. Boubaris, and Nick P. Papanikolaou. 2021. "Ancillary Services in Active Distribution Networks: A Review of Technological Trends from Operational and Online Analysis Perspective." *Renewable and*

Sustainable Energy Reviews 147: 111198. doi:https://doi.org/10.1016/j.rser.2021.111198. https://www.sciencedirect.com/science/article/pii/S136403212100486X.

[5] Tuttelberg, K., J. Kilter, D. Wilson, and K. Uhlen. 2018. "Estimation of Power System Inertia from Ambient Wide Area Measurements." *IEEE Transactions on Power Systems* 33 (6): 7249-7257. doi:10.1109/TPWRS.2018.2843381.

[6] Ashton, P. M., C. S. Saunders, G. A. Taylor, A. M. Carter, and M. E. Bradley. 2015. "Inertia Estimation of the GB Power System using Synchrophasor Measurements." *IEEE Transactions on Power Systems* 30 (2): 701-709. doi:10.1109/TPWRS.2014.2333776.

[7] Du, P. and J. Matevosyan. 2018. "Forecast System Inertia Condition and its Impact to Integrate More Renewables." *IEEE Transactions on Smart Grid* 9 (2): 1531-1533. doi:10.1109/TSG.2017.2662318.

[8] Allella, F., E. Chiodo, G. M. Giannuzzi, D. Lauria, and F. Mottola. 2020. "On-Line Estimation Assessment of Power Systems Inertia with High Penetration of Renewable Generation." *IEEE Access* 8: 62689-62697. doi:10.1109/ACCESS.2020.2983877.

[9] KUIVANIEMI M., LAASONEN M., K. Elkington, A. Danell, N. Modig, A. I. Bruseth, E. A. Jansson, and E. Ørum. 2015. "Estimation of System Inertia in the Nordic Power System using Measured Frequency Disturbances."CIGRÉ, 2015.

[10] Wilson, D., J. Yu, N. Al-Ashwal, B. Heimisson, and V. Terzija. 2019. "Measuring Effective Area Inertia to Determine Fast-Acting Frequency Response Requirements." *International Journal of Electrical Power & Energy Systems* 113: 1-8. doi:https://doi.org/10.1016/j.ijepes.2019.05.034. https://www.sciencedirect.com/science/article/pii/S0142061519304892.

[11] Phurailatpam, C., Z. H. Rather, B. Bahrani, and S. Doolla. 2021. "Estimation of Non-Synchronous Inertia in AC Microgrids." *IEEE Transactions on Sustainable Energy*: 1. doi:10.1109/TSTE.2021.3070678.

[12] Azizi, S., M. Sun, G. Liu, and V. Terzija. 2020. "Local Frequency-Based Estimation of the Rate of Change of Frequency of the Center of Inertia." *IEEE Transactions on Power Systems* 35 (6): 4948-4951. doi:10.1109/TPWRS.2020.3014818.

[13] Pagnier, L. and P. Jacquod. 2019. "Optimal Placement of Inertia and Primary Control: A Matrix Perturbation Theory Approach." *IEEE Access* 7: 145889-145900. doi:10.1109/ACCESS.2019.2945475.

[14] Zhao, J., M. Netto, Z. Huang, S. S. Yu, A. Gómez-Expósito, S. Wang, I. Kamwa, et al. 2021. "Roles of Dynamic State Estimation in Power System Modeling, Monitoring and Operation." *IEEE Transactions on Power Systems* 36 (3): 2462-2472. doi:10.1109/TPWRS.2020.3028047.

[15] Heylen, Evelyn, Fei Teng, and Goran Strbac. 2021. "Challenges and Opportunities of Inertia Estimation and Forecasting in Low-Inertia Power Systems." *Renewable and Sustainable*

Energy Reviews 147: 111176. doi:https://doi.org/10.1016/j.rser.2021.111176. https://www.sciencedirect.com/science/article/pii/S1364032121004652.

[16] Cai, G., B. Wang, D. Yang, Z. Sun, and L. Wang. 2019. "Inertia Estimation Based on Observed Electromechanical Oscillation Response for Power Systems." *IEEE Transactions on Power Systems* 34 (6): 4291-4299. doi:10.1109/TPWRS.2019.2914356.

[17] Guo, S., S. Norris, and J. Bialek. 2014. "Adaptive Parameter Estimation of Power System Dynamic Model using Modal Information." *IEEE Transactions on Power Systems* 29 (6): 2854-2861. doi:10.1109/TPWRS.2014.2316916.

[18] Fan, L., Z. Miao, and Y. Wehbe. 2013. "Application of Dynamic State and Parameter Estimation Techniques on Real-World Data." *IEEE Transactions on Smart Grid* 4 (2): 1133-1141. doi:10.1109/TSG.2012.2230031.

[19] Inoue, T., H. Taniguchi, Y. Ikeguchi, and K. Yoshida. 1997. "Estimation of Power System Inertia Constant and Capacity of Spinning-Reserve Support Generators using Measured Frequency Transients." *IEEE Transactions on Power Systems* 12 (1): 136-143. doi:10.1109/59.574933.

[20] Wall, P. and V. Terzija. 2014. "Simultaneous Estimation of the Time of Disturbance and Inertia in Power Systems." *IEEE Transactions on Power Delivery* 29 (4): 2018-2031. doi:10.1109/TPWRD.2014.2306062.

[21] Schiffer, J., P. Aristidou, and R. Ortega. 2019. "Online Estimation of Power System Inertia using Dynamic Regressor Extension and Mixing." *IEEE Transactions on Power Systems* 34 (6): 4993-5001. doi:10.1109/TPWRS.2019.2915249.

[22] Zografos, Dimitrios, Mehrdad Ghandhari, and Robert Eriksson. 2018a. "Power System Inertia Estimation: Utilization of Frequency and Voltage Response After a Disturbance." *Electric Power Systems Research* 161: 52-60. doi:https://doi.org/10.1016/j.epsr.2018.04.008. https://www.sciencedirect.com/science/article/pii/S037877961830107X.

[23] Azizipanah-Abarghooee, R., M. Malekpour, M. Paolone, and V. Terzija. 2019. "A New Approach to the Online Estimation of the Loss of Generation Size in Power Systems." *IEEE Transactions on Power Systems* 34 (3): 2103-2113. doi:10.1109/TPWRS.2018.2879542.

[24] Yang, D., B. Wang, J. Ma, Z. Chen, G. Cai, Z. Sun, and L. Wang. 2020. "Ambient-Data-Driven Modal-Identification-Based Approach to Estimate the Inertia of an Interconnected Power System." *IEEE Access* 8: 118799-118807. doi:10.1109/ACCESS.2020.3004335.

[25] Best, R. J., P. V. Brogan, and D. J. Morrow. 2021. "Power System Inertia Estimation using HVDC Power Perturbations." *IEEE Transactions on Power Systems* 36 (3): 1890-1899. doi:10.1109/TPWRS.2020.3028614.

[26] S. Shah and V. Gevorgian. 2019. "Impedance-Based Characterization of Power System Frequency Response.". doi:10.1109/PESGM40551.2019.8974031.

[27] A. Schmitt and B. Lee. 2017. "Steady-State Inertia Estimation using a Neural Network Approach with Modal Information.". doi:10.1109/PESGM.2017.8274640.

[28] *Development and Validation of Artificial Neural Network-Based Tools for Forecasting of Power System Inertia with Wind Farms Penetration*. Vol. 14. doi:10.1109/JSYST.2020.3017640E. S. N. R. Paidi, H. Marzooghi, J. Yu, et al.

[29] *Switching Markov Gaussian Models for Dynamic Power System Inertia Estimation*. Vol. 31. doi:10.1109/TPWRS.2015.2501458X. Cao, B. Stephen, I. F. Abdulhadi, et al.

[30] *Identification and Predictive Analysis of a Multi-Area WECC Power System Model using Synchrophasors*. Vol. 8. doi:10.1109/TSG.2016.2531637G. Chavan, M. Weiss, A. Chakrabortty, et al.

[31] Panda, R. K., A. Mohapatra, and S. C. Srivastava. 2020. "Online Estimation of System Inertia in a Power Network Utilizing Synchrophasor Measurements." *IEEE Transactions on Power Systems* 35 (4): 3122-3132. doi:10.1109/TPWRS.2019.2958603.

[32] Yang, D., B. Wang, G. Cai, Z. Chen, J. Ma, Z. Sun, and L. Wang. 2021. "Data-Driven Estimation of Inertia for Multiarea Interconnected Power Systems using Dynamic Mode Decomposition." *IEEE Transactions on Industrial Informatics* 17 (4): 2686-2695. doi:10.1109/TII.2020.2998074.

[33] Lugnani, Lucas, Daniel Dotta, Christoph Lackner, and Joe Chow. 2020. "ARMAX-Based Method for Inertial Constant Estimation of Generation Units using Synchrophasors." *Electric Power Systems Research* 180: 106097. doi:https://doi.org/10.1016/j.epsr.2019.106097. https://www.sciencedirect.com/science/article/pii/S037877961930416X.

[34] Liu, M., J. Chen, and F. Milano. 2021. "On-Line Inertia Estimation for Synchronous and Non-Synchronous Devices." *IEEE Transactions on Power Systems* 36 (3): 2693-2701. doi:10.1109/TPWRS.2020.3037265.

[35] Zeng, F., J. Zhang, Y. Zhou, and S. Qu. 2020. "Online Identification of Inertia Distribution in Normal Operating Power System." *IEEE Transactions on Power Systems* 35 (4): 3301-3304. doi:10.1109/TPWRS.2020.2986721.

[36] Zeng, F., J. Zhang, G. Chen, Z. Wu, S. Huang, and Y. Liang. 2020. "Online Estimation of Power System Inertia Constant Under Normal Operating Conditions." *IEEE Access* 8: 101426-101436. doi:10.1109/ACCESS.2020.2997728.

[37] *Generator Dynamic Model Validation and Parameter Calibration using Phasor Measurements at the Point of Connection*. Vol. 28. doi:10.1109/TPWRS.2013.2251482Z. Huang, P. Du, D. Kosterev, et al.

[38] Fan, Lingling and Yasser Wehbe. 2013. "Extended Kalman Filtering Based Real-Time Dynamic State and Parameter Estimation using PMU Data." *Electric Power Systems Research* 103: 168-177. doi:https://doi.org/10.1016/j.epsr.2013.05.016. https://www.sciencedirect.com/science/article/pii/S0378779613001442.

[39] Ariff, M. A. M., B. C. Pal, and A. K. Singh. 2015. "Estimating Dynamic Model Parameters for Adaptive Protection and Control in Power System." *IEEE Transactions on Power Systems* 30 (2): 829-839. doi:10.1109/TPWRS.2014.2331317.

[40] Zhao, J., Y. Tang, and V. Terzija. 2019. "Robust Online Estimation of Power System Center of Inertia Frequency." *IEEE Transactions on Power Systems* 34 (1): 821-825. doi:10.1109/TPWRS.2018.2879782.

[41] Wang, B., D. Yang, G. Cai, J. Ma, Z. Chen, and L. Wang. 2020. "Online Inertia Estimation using Electromechanical Oscillation Modal Extracted from Synchronized Ambient Data." *Journal of Modern Power Systems and Clean Energy*: 1-4. doi:10.35833/MPCE.2020.000105.

[42] Sun, M., Y. Feng, P. Wall, S. Azizi, J. Yu, and V. Terzija. 2019. "On-Line Power System Inertia Calculation using Wide Area Measurements." *International Journal of Electrical Power & Energy Systems* 109: 325-331. doi:https://doi.org/10.1016/j.ijepes.2019.02.013. https://www.sciencedirect.com/science/article/pii/S0142061518336640.

[43] Tavakoli, M. Reza Bank, Michael Power, Lisa Ruttledge, and Damian Flynn. 2012. "Load Inertia Estimation using White and Grey-Box Estimators for Power Systems with High Wind Penetration." *IFAC Proceedings Volumes* 45 (21): 399-404. doi:https://doi.org/10.3182/20120902-4-FR-2032.00071. https://www.sciencedirect.com/science/article/pii/S1474667016320031.

[44] He, W., X. Yuan, and J. Hu. 2017. "Inertia Provision and Estimation of PLL-Based DFIG Wind Turbines." *IEEE Transactions on Power Systems* 32 (1): 510-521. doi:10.1109/TPWRS.2016.2556721.

[45] *Inertia Estimation of Wind Power Plants Based on the Swing Equation and Phasor Measurement Units*. Vol. 8. doi:10.3390/app8122413Omar Beltran, Rafael Peña, Juan Segundo, et al.

[46] Lu, J., D. Zhao, Y. Xu, J. Wang, and X. Yuan. 2020. "Evaluation of Available Inertia of Wind Farms Based on Mixed Copula.". doi:10.1109/ACPEE48638.2020.9136495.

[47] *Pushing the Limits: Europe's New Grid: Innovative Tools to Combat Transmission Bottlenecks and Reduced Inertia*. Vol. 13. doi:10.1109/MPE.2014.2363534W. Winter, K. Elkington, G. Bareux, et al.

[48] ENTSO-e. 2018. *Future System Inertia*: ENTSO-e.

[49] Glavic, Mevludin. 2016. *Dynamic Equivalents of Active Distribution Networks: A Short Review*. University of Liege.

[50] Yu, Y., M. A. El-sharkawi, and M. D. Wvong. 1979. "Estimation of Unknown Large Power System Dynamics." *IEEE Transactions on Power Apparatus and Systems* PAS-98 (1): 279-289. doi:10.1109/TPAS.1979.319529.

[51] X. Feng, Z. Lubosny, and J. Bialek. 2006. "Dynamic Equivalencing of Distribution Network with High Penetration of Distributed Generation.". doi:10.1109/UPEC.2006.367521.

[52] *Validation of Equivalent Dynamic Model of Active Distribution Network Cell*. Vol. 28. doi:10.1109/TPWRS.2012.2227844J. V. Milanović and S. Mat Zali.

[53] *An Active Distribution Network Equivalent Derived from Large-Disturbance Simulations with Uncertainty*. Vol. 11. doi:10.1109/TSG.2020.2999114G. Chaspierre, G. Denis, P. Panciatici, et al.

[54] *Experimental Validation of a Dynamic Equivalent Model for Microgrids*. Vol. 57. doi:10.1109/TIA.2021.3064522F. Conte, F. D'Agostino, S. Massucco, et al.

[55] Phurailatpam, C., Z. H. Rather, B. Bahrani, and S. Doolla. 2020. "Measurement-Based Estimation of Inertia in AC Microgrids." *IEEE Transactions on Sustainable Energy* 11 (3): 1975-1984. doi:10.1109/TSTE.2019.2948224.

[56] Sun, Qicong, Yan Li, and Jason Philhower. 2021. "Data-Driven Resilience Analysis of Power Grids." *Global Energy Interconnection* 4 (1): 104-114. doi:https://doi.org/10.1016/j.gloei.2021.03.010. https://www.sciencedirect.com/science/article/pii/S2096511721000293.

[57] Zografos, Dimitrios, Mehrdad Ghandhari, and Robert Eriksson. 2018b. "Power System Inertia Estimation: Utilization of Frequency and Voltage Response After a Disturbance." *Electric Power Systems Research* 161: 52-60. doi:https://doi.org/10.1016/j.epsr.2018.04.008. https://www.sciencedirect.com/science/article/pii/S037877961830107X.

[58] Kontis, Eleftherios O., Ioanna D. Pasiopoulou, Dimosthenis A. Kirykos, Theofilos A. Papadopoulos, and Grigorios K. Papagiannis. 2021. "Estimation of Power System Inertia: A Comparative Assessment of Measurement-Based Techniques." *Electric Power Systems Research* 196: 107250. doi:https://doi.org/10.1016/j.epsr.2021.107250. https://www.sciencedirect.com/science/article/pii/S0378779621002315.

[59] Chassin, D. P., Z. Huang, M. K. Donnelly, C. Hassler, E. Ramirez, and C. Ray. 2005. "Estimation of WECC System Inertia using Observed Frequency Transients." *IEEE Transactions on Power Systems* 20 (2): 1190-1192. doi:10.1109/TPWRS.2005.846155.

[60] Bian, Y., H. Wyman-Pain, F. Li, R. Bhakar, S. Mishra, and N. P. Padhy. 2018. "Demand Side Contributions for System Inertia in the GB Power System." *IEEE Transactions on Power Systems* 33 (4): 3521-3530. doi:10.1109/TPWRS.2017.2773531.

[61] GE. "Effective Inertia.", https://www.ge.com/digital/sites/default/files/download_assets/effective-inertia-datasheet-ge-grid-analytics.pdf.

[62] Federico Milano and Alvaro Ortega Manjavacas. 2020. *Dynamic State Estimation*. - Frequency Variations in Power Systems: Modeling, State Estimation, and Control. doi:10.1002/9781119551881.ch8.

[63] *Estimation of Radial Power System Transfer Path Dynamic Parameters using Synchronized Phasor Data*. Vol. 23. doi:10.1109/TPWRS.2008.919315J. H. Chow, A. Chakrabortty, L. Vanfretti, et al.

[64] Hartono, J., P. A. Aditya Pramana, A. A. Kusuma, and B. S. Munir. 2019. "Power System Inertia Estimation Based on Frequency Measurement.". doi:10.1109/APCoRISE46197.2019.9318909.

[65] *A Bayesian Approach for Parameter Estimation with Uncertainty for Dynamic Power Systems*. Vol. 32. doi:10.1109/TPWRS.2016.2625277N. Petra, C. G. Petra, Z. Zhang, et al.

[66] Vieyra, Natanael, Paul Maya, and Luis M. Castro. 2020. "Effective Dynamic State Estimation Algorithm for Islanded Microgrid Structures Based on Singular Perturbation Theory." *Electric Power Systems Research* 187: 106455. doi:https://doi.org/10.1016/j.epsr.2020.106455. https://www.sciencedirect.com/science/article/pii/S0378779620302595.

[67] *A Robust Iterated Extended Kalman Filter for Power System Dynamic State Estimation*. Vol. 32. doi:10.1109/TPWRS.2016.2628344J. Zhao, M. Netto and L. Mili.

[68] Wang, Xueyuan, Junbo Zhao, Vladimir Terzija, and Shaobu Wang. 2020. "Fast Robust Power System Dynamic State Estimation using Model Transformation." *International Journal of Electrical Power & Energy Systems* 114: 105390. doi:https://doi.org/10.1016/j.ijepes.2019.105390. https://www.sciencedirect.com/science/article/pii/S0142061519316539.

[69] *Online Identification of Power System Equivalent Inertia Constant*. Vol. 64. doi:10.1109/TIE.2017.2698414J. Zhang and H. Xu.

[70] *Maximum Frequency Deviation Calculation in Small Isolated Power Systems*. Vol. 24. doi:10.1109/TPWRS.2009.2030399I. Egido, F. Fernandez-Bernal, P. Centeno, et al.

[71] Berry, B. B. 2019. "Inertia Estimation Methodologies Vs Measurement Methodology: Impact on
System Operations."CIGRÉ, 2019.

[72] Wang, Y., H. Silva-Saravia, and H. Pulgar-Painemal. 2017. "Estimating Inertia Distribution to Enhance Power System Dynamics.". doi:10.1109/NAPS.2017.8107383.

[73] Pulgar-Painemal, H., Y. Wang, and H. Silva-Saravia. 2018. "On Inertia Distribution, Inter-Area Oscillations and Location of Electronically-Interfaced Resources." *IEEE Transactions on Power Systems* 33 (1): 995-1003. doi:10.1109/TPWRS.2017.2688921.

[74] Xiao, Y., X. Lin, and Y. Wen. 2019. "A Framework for Assessing the Inertia Distribution of Power Systems.". doi:10.1109/EI247390.2019.9061937.

[75] Brahma, D. and N. Senroy. 2021. "Spatial Distribution of Grid Inertia and Dynamic Flexibility: Approximations and Applications." *IEEE Transactions on Power Systems* 36 (4): 3465-3474. doi:10.1109/TPWRS.2021.3050085.

[76] You, S., Y. Liu, G. Kou, X. Zhang, W. Yao, Y. Su, S. W. Hadley, and Y. Liu. 2018. "Non-Invasive Identification of Inertia Distribution Change in High Renewable Systems using Distribution Level PMU." *IEEE Transactions on Power Systems* 33 (1): 1110-1112. doi:10.1109/TPWRS.2017.2713985.

[77] Lara-Jimenez, Jose, Juan M. Ramırez, and Fernando Mancilla-David. 2017. "Allocation of PMUs for Power System-Wide Inertial Frequency Response Estimation." *IET Generation, Transmission & Distribution* 11 (11): 2902-2911. doi:https://doi.org/10.1049/iet-gtd.2016.1951. https://doi.org/10.1049/iet-gtd.2016.1951.

[78] *Fast and Accurate Frequency Response Estimation for Large Power System Disturbances using Second Derivative of Frequency Data*. Vol. 35. doi:10.1109/TPWRS.2020.2977504W. Wang, W. Yao, C. Chen, et al.

[79] Shams, N., P. Wall, and V. Terzija. 2019. "Active Power Imbalance Detection, Size and Location Estimation using Limited PMU Measurements." *IEEE Transactions on Power Systems* 34 (2): 1362-1372. doi:10.1109/TPWRS.2018.2872868.

[80] Fernández-Guillamón, Ana, Antonio Vigueras-Rodríguez, and Ángel Molina-García. 2019. "Analysis of Power System Inertia Estimation in High Wind Power Plant Integration Scenarios." *IET Renewable Power Generation* 13 (15): 2807-2816. doi:https://doi.org/10.1049/iet-rpg.2019.0220. https://doi.org/10.1049/iet-rpg.2019.0220.

[81] Vorobev, P., D. M. Greenwood, J. H. Bell, J. W. Bialek, P. C. Taylor, and K. Turitsyn. 2019. "Deadbands, Droop, and Inertia Impact on Power System Frequency Distribution." *IEEE Transactions on Power Systems* 34 (4): 3098-3108. doi:10.1109/TPWRS.2019.2895547.

[82] Sigrist, Lukas and Luis Rouco. 2017. "An Induction Motor Model for System Frequency Response Models." *International Transactions on Electrical Energy Systems* 27 (11): e2413. doi:https://doi.org/10.1002/etep.2413. https://doi.org/10.1002/etep.2413.

[83] P. M. Ashton, G. A. Taylor, A. M. Carter, M. E. Bradley, and W. Hung. 2013. "Application of Phasor Measurement Units to Estimate Power System Inertial Frequency Response.". doi:10.1109/PESMG.2013.6672671.